UNIVERSITY OF OKLAHOMA

GRADUATE COLLEGE

FAULT DETECTION AND DIAGNOSIS OF AIR HANDLING UNIT IN HVAC SYSTEM USING CLOUD-BASED DATA LOGGING SYSTEM

A THESIS

SUBMITTED TO THE GRADUATE FACULTY

in partial fulfillment of the requirements for the

Degree of

MASTER OF SCIENCE

By

DAVID LEE
Norman, Oklahoma
2019

FAULT DETECTION AND DIAGNOSIS OF AIR HANDLING UNIT IN HVAC SYSTEM USING CLOUD-BASED DATA LOGGING SYSTEM

A THESIS APPROVED FOR THE
SCHOOL OF AEROSPACE AND MECHANICAL ENGINEERING

BY

Dr. Li Song, Chair

Dr. Jie Cai

Dr. Wilson E. Merchán-Merchán

Acknowledgements

I would like to give special thanks to all the people who supported and guided me throughout the completion of this thesis.

I thank my adviser, Dr. Li Song, for inspiring me to pursue a higher education. Her support led me to finding my life's passion in the field of HVAC systems and energy efficient building design and discovering the ASHRAE community to keep advancing my understanding and improving future engineering design and practices. She encouraged and enabled me to finish my Master's degree with scholarships. Not only was she challenging and motivating but personal and caring, always understanding and listening to what I was thinking; I could easily tell that she genuinely loved what she does and is very talented. I am eternally thankful for your mentorship and guidance in academic and personal career life. I also like to thank my committee members, Dr. Jie Cai and Dr. Wilson Merchan-Merchan. Thank you very much for your time, advice, and teachings throughout my education of B.S and M.S. in the University of Oklahoma. Also, special thanks to all AME staff- Bethany Burkland, Melissa Foster, Billy Mays, and Greg Williams. I thank my colleagues working in the BEEL (Building Energy Efficiency Laboratory)- Junke Wang, Zhimin Jiang, Tianyang Zhao, and Spencer Hinkle for your support. I appreciate Dr. Mrinal Saha and the AME Graduate Student Society for the opportunity to develop networking and expand my knowledge in other research fields of Mechanical Engineering science. I acknowledge the financial scholarship received from ASHRAE (via Oklahoma City Community Foundation Scholarship) and OU Graduate College.

I express my gratitude to my friends and family who both comforted and propelled me to achieve what I never thought I could in my life. I thank my beautiful best friend, Megan Gentry. Thank you for helping me become a better man every day. You influence me more than you can ever imagine. I love you and thank you. I am who I am today thanks to my parents and brothers, Jong-Oh Lee, Yeon-Ok Lee, John and Jeremiah Lee. Thank you for being the best family I could ever have in my life. I love you eternally.

Table of Contents

List of Tables

List of Figures

Nomenclature

T_{oa}	Outside air temperature [^{o}F or ^{o}C]
T_{ra}	Return air temperature [^{o}F or ^{o}C]
T_{ma}	Mixed air temperature [^{o}F or ^{o}C]
T_{sa}	Supply air temperature [^{o}F or ^{o}C]
RH_{oa}	Relative humidity [%]
$T_{w,o}$	Chiller water outlet temperature [^{o}F or ^{o}C]
$T_{w,i}$	Chiller water inlet temperature [^{o}F or ^{o}C]
$P_{w,o}$	Chiller water outlet pressure [psi or Pa]
$P_{w,i}$	Chiller water inlet pressure [lbm/hr or kg/s]
P_{diff}	Fan differential static pressure [inch. Wg or Pa]
V_{valve}	Output signal of control valve [V]
V_{rpm}	Output signal of fan speed [V]
f_{rpm} or ω	Fan speed [rpm]
V_{power}	Output signal of fan power [V]
Q	Volumetric airflow rate [$(ft^3/min)^2$ or CFM or (m^3/s)]
$\dot{m}_{oa}$	Mass flow rate of outside air [lbm/hr or kg/s]
$\dot{m}_{sa}$	Mass flow rate of supply air [lbm/hr or kg/s]
$\dot{m}_{ma}$	Mass flow rate of mixed air [lbm/hr or kg/s]
i_{oa}	Outside air enthalpy [Btu/lbm or J/kg]
i_{ra}	Return air enthalpy [Btu/lbm or J/kg]
i_{ma}	Mixed air enthalpy [Btu/lbm or J/kg]

W	Absolute humidity [g/m^3]
α	Outside air fraction [%]
$\dot{q}_{air-side}$	Air-side heat transfer rate [Btu/hr or W]
$\dot{q}_{water-side}$	Water-side heat transfer rate [Btu/hr or W]
U	heat transfer coefficient [W/K-m^2 or Btu/hr-F-ft^2]
A	Heat exchange area [m^2 or ft^2]
$LMTD$	Logarithmic mean temperature difference
H_{fan} or H	Fan head [inch. Wg or Pa]
kW	Fan input power consumption [kW]
P	Fan power [HP or kW]
S	System resistance coefficient [inch.wg / (ft^3/min)^2 or Pa/(m^3/s)]

Abstract

This project encompasses the engineering principles of design and testing of the implementation of a fault detection and diagnosis (FDD) using cloud-based data logging system on Heating, Ventilation, and Air Conditioning (HVAC) system. The data acquisition system is a compact measurement system made by Paragon Robotics that handles data from sensors, measurement hardware, and a computer with appropriate software to record four different categories of measurements: (1) temperature and humidity of outside air, (2) temperature of return, mixed, and supply air, (3) cooling oil valve operation measurements, and (4) supply air fan operation measurements.

The project includes the design process of the equipment and installation of electrical and mechanical components needed for a functioning system on an Air Handling Unit (AHU) that serves a building in the University of Oklahoma. Tests of baseline operation are conducted to collect weeks of data after calibration. The system is verified with engineering fundamental Models to ensure robustness for fault detection and diagnosis. Common faults of AHU are evaluated and selected to be simulated into the system for days with faulty operation data. Qaulitative rule-based or physics-based FDD technique is used to detect and diagnose the system with data collected during operations of faults.

Chapter 1: Introduction

This chapter introduces the fundamental basis and background information of Heating, Ventilation, and Air Conditioning (HVAC) System, the Air Handling Unit (AHU) and Fault Detection and Diagnosis (FDD). Then, it provides the overview of the challenges and objectives of the research project.

1.1 Background

In many buildings, human thermal and health comfort is achieved with development and industrialization of year-round control of indoor environment. Heating, Ventilation, and Air Conditioning (HVAC) systems produce the temperature, humidity, and air quality that humans need to improve health and productivity in their lives. Now, the HVAC system has become so important for every residential, commercial, industrial, and institutional buildings in the industrial countries of the world.

In the early stages of the advancement of HVAC technology, energy consumption was not considered as a vital factor due to the abundance and inexpensive cost of fuel and unknown issues of climate change related to consumption. As the usage of HVAC system escalated in the United States during the 1970s, the energy crisis hit. The Department of Energy was launched in effort to re-design and invent energy-efficient buildings. Although current modern air conditions use about 50 percent less energy compared to 1970's [1], the data indicates nearly 40 percent of total U.S. energy consumption was consumed by the residential and commercial buildings in 2017 [2]. According to a study in 2001, HVAC systems use 20 to 60 percent of the total energy consumed by buildings [3].

The primary function of building energy systems is to meet thermal comfort, utilizing energy transfer in most efficient method. Other aims can be to provide required amount of suitable ventilation air to prevent illnesses and allergies and control humidity to eliminate mold effect on human health and mold damages to buildings. HVAC systems are rapidly growing as modern buildings are necessary to meet performance requirements and codes. Computers and building automation systems (BAS) are integrated for operational controls of the buildings enabling sharing of data between systems and control indoor environment to ensure adequate indoor climate and healthy climate and healthy conditions for occupants.

1.1.1 Heating, Ventilating, and Air-conditioning (HVAC) Systems

HVAC systems vary in their configurations and types depending on the design and the operational purpose. A diagram of a typical HVAC system with central plant is presented in Figure 1.1. A system in the example is comprised of fans or air handling units (AHU) for moving air with associated dampers and filters, pumps for moving heated or chilled water and appropriate control valves, heat exchangers for transferring energy from one fluid stream to another, flow measuring and control devices and chillers and furnace or boiler equipment, and a cooling Tower. The central plant, with a main boiler and chiller, serves as the main source of energy distribution to multiple air handling units. The air handling system is an assembly of fans, heating and cooling coils, filters, humidifiers, and controlling dampers. Then, the air is transferred through ducts all governed by terminal units.

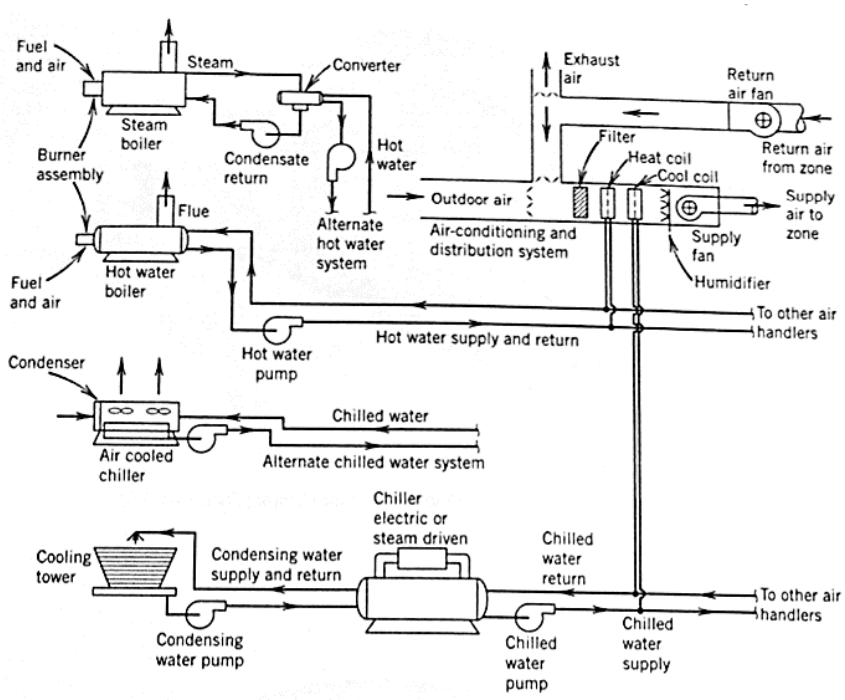

Figure 1.1: Schematic of the equipment providing heating or cooling fluid to air handlers in typical all-air commercial HVAC systems

(source: Heating, Ventilating, and Air Conditioning by Faye McQuiston)

Air Handling Unit (AHU) is a crucial component of the heating, ventilation, and air conditioning (HVAC) systems for the connections to primary heating and cooling coils and preservation of indoor air quality with outside air. Each building also has various range of the units, all dependent on the size and layout of the building. A fluid, usually water, carries energy away from the cooling coil (heat exchanger) in the air handler to a chiller or chillers. The loads of the coils determine the electricity and gas consumed by the central plant. So, AHU conditions directly translate to the quantity of the energy consumption.

Failures of HVAC systems are caused by improper installation, inadequate maintenance, or equipment failure. Faults can prevent the buildings to achieve expected energy efficiency. More and more HVAC experts pay attention to “fault detection and

diagnosis". Fault Detection and Diagnosis (FDD) analysis refers to analytical tool of techniques used to detect and diagnose these faults. FDD method is used in all engineering industries such as aerospace, materials science, chemical processing, photovoltaic systems, controls systems design and more. Nevertheless, this set of techniques is used in building operation systems for optimization.

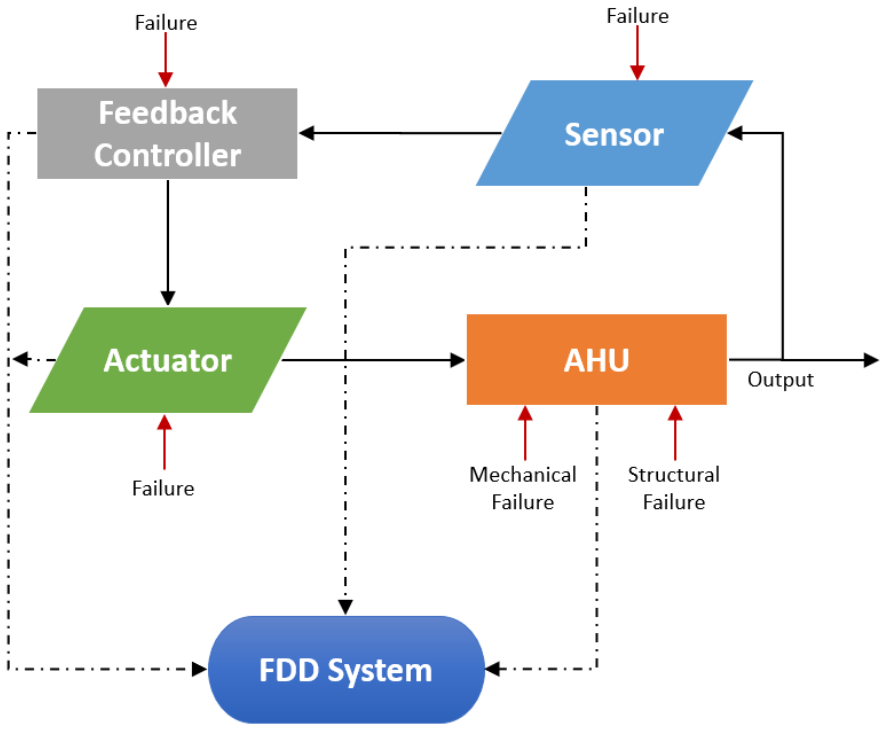

Figure 1.2: The basic FDD framework

FDD can improve building energy consumption, operations and maintenance, an effective control over air quality and environment of the indoor spaces [4]. In fact, the estimated energy savings is at 10-40% depending on the age and condition of the equipment, maintenance practices, climate, and building use [5] [6] [7] [8]. FDD allows identification of minor problems before it becomes major and severe which means equipment can be repaired, extending the service life. Also, BAS systems provide sophisticated control systems with data communication, computing, and data

visualization technologies. This led to advancement of Automated Fault Detection and Diagnosis (AFDD) enabling it to automatically detect faults, diagnose their causes at an early stage and prevent further damage and/or energy loss.

1.2 Literature review

Due to the rapid growth in this energy saving strategies, research in FDD analysis has been necessary and in demand. Two baseline methods to optimize energy consumption and achieving other operational targets are top-down (system level) and bottom-up (component level) approaches [9]. Top-down approach deals with monitoring and targeting approaches, energy performance indicators and performance dashboards to manage site energy consumption. This method is mostly performed by industrial and large/multi-commercial sites. For example, if building energy use exceeds its expected value by an amount considered to be significant, top-down reasoning would be used to navigate down through the hierarchy and isolate the most probable cause for the exceeding energy use [10]. Dodier and Kreider presents a whole-building FDD approach for energy-based problem detection [11].

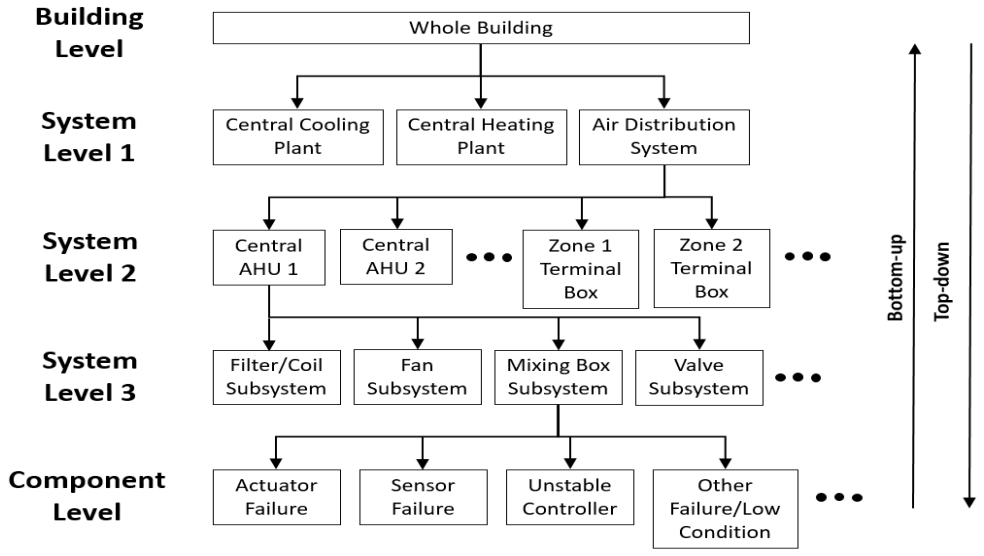

Figure 1.3: Top-down and bottom-up of FDD building system

On the contrary, bottom-up method involves from breakdown maintenance of key AHU components, such as fans and filters, to time-based maintenance and management of the components. Furthermore, it also encompasses future preventative solution by prognostic Modelling options for remaining useful life estimation of equipment [12]. Currently, there are numerous studies of FDD analysis systems in buildings on the component-level.

The methods of FDD analysis in bottom-up approach can be classified into three categories: Model-based, rule-based, and data-driven methods. Model-based FDD methods, or black-box method, utilize physical or mathematical Models which are based on understandings of the process concerned. Then, comparison of the real process and the predictive Model renders detection and diagnosis of the faults [13] [14] [15]. With experiential rules and proper process of reasoning, fault can be diagnosed through checking whether the system is in appliance to the rules. This method is rule-based methods [16] [17]. Lastly, the data-driven FDD methods make use of historical statistics to capture the quantitative correlations among system variables. This method was adopted due to abundant data available from Modern BAS. The data-driven methods developed neural network, wavelet analysis, and the statistical methods such as principal component analysis (PCA), Fisher discriminant analysis, and pattern matching method [18] [19] [20] [21] [22] [23].

Model-based methods usually produce the most reliable results when the physical equations and algorithms are precisely formulated. However, it is hardly possible to build the mathematical Models because HVAC systems are highly complex, multivariable, nonlinear, and comprised of heat and mass transfer. In regard to the rule-

based FDD methods, it is comparatively easier to develop the rules and reasoning processes. But the rules are very specific to individual systems and types of faults. The diagnosis will fail if the fault is beyond the rule database. The data-driven method is applicable in the systems with already ample operation data and easy to obtain [24].

1.3 Problem Statement

Research and advancement of FDD analysis in HVAC systems are on the rise with numerous applications and cases of impactful energy savings, as it is described in the background. Since FDD is a new topic of studies, compared to the long years of HVAC industry, most FDD systems are built-in in smart HVAC systems with BAS systems, or other intelligent controllers, in new projects and modern buildings, which are limited by computational capacity and the amount of metered data available. The Internet is an infrastructure for information and communications technologies. HVAC systems must keep advancing with modern technology by the adoption of more advanced information technology, using internet to store, retrieve, transmit, and manipulate data. Cloud-based wireless FDD system presents portable, reliable, and cost-effective method with greater storage capacity of easily accessible real-time data. The cloud servers also allow quick interchangeable monitoring software for data analysis at any time. There are not many documented case studies to validate the effectiveness of using cloud-based data logging system for FDD practices. [25] [26]

1.4 Objective of thesis project

The objective of this thesis is to develop the FDD system with cloud-based data logging system for an AHU that serves a building in the University of Oklahoma. This project includes:

- Consideration of physical boundaries and schedules of AHU equipment.
- Design, locating, and installation of wireless cloud-based data logging system
- Data collection and evaluation of optimal performance/condition of AHU
- Introduction of various frequent faults and analysis of created fault
- Diagnosis of fault by data analysis and communication with users of FDD.

Due to the cloud-based technology, the system will be modular to other systems. This means the FDD Model must be able to recognize other types of systems. The heavy rule-based/model-based FDD Model is decided to see the robustness of the cloud-based system.

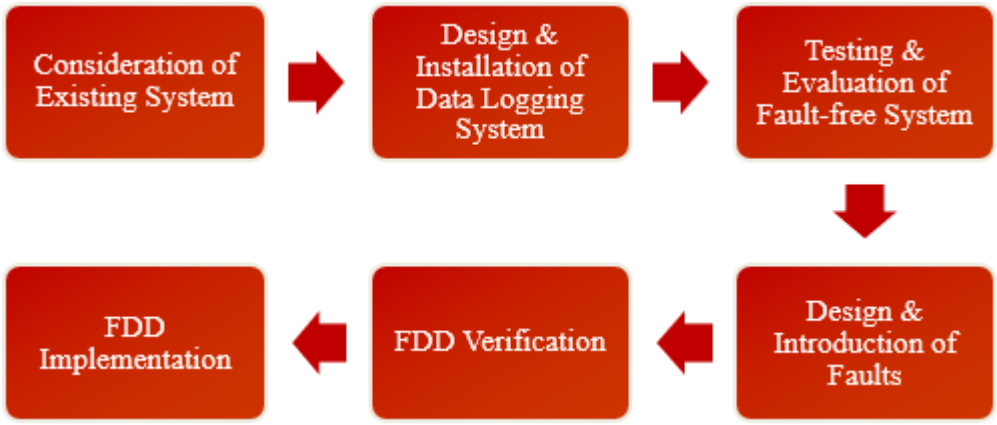

Figure 1.4: Flow layout of the project

1.5 Overview of thesis project

Chapter 1 introduces the basic information of HVAC system and its component, AHU. Then, it explains the emergence of FDD or AFDD with BAS through the literature reviews and the three different categories of methodologies of the latest FDD analysis. This chapter also presents the problem statement and objective of this project.

Chapter 2 gives a brief explanation of the data logging system. It proposes the design process and selection of the cloud-based devices. In the chapter, the installation

of the devices is carefully described in detail. Data of optimal performance/condition of AHU is collected and analyzed with engineering principles.

Chapter 3 introduces the design process of FDD. It demonstrates lists of various frequent faults of AHU systems. The chapter demonstrates the introduction of three selected faults to the system. It describes the data collection and analysis with the FDD. The effectiveness of the FDD system using cloud-based data logging system is presented.

Chapter 4 summaries the main conclusions and achievements of the research of this project and suggests a collective of future works to improve the application of proposed FDD method in practices.

Chapter 2: Cloud-Based Data Logging System

In this project, a typical air handling unit located in a building of the University of Oklahoma is studied. To install the FDD system into the AHU, a robust data logging system is necessary. Data logging system is an essential tool to analyze any type of systems. Data acquisition is the process of measuring an electrical or physical property such as voltage, current, temperature, pressure, or sound with a computer. This system consists of sensors, data logging device, and computer with programmable software. Figure 2.1 explains a simple process and components of the data logging system.

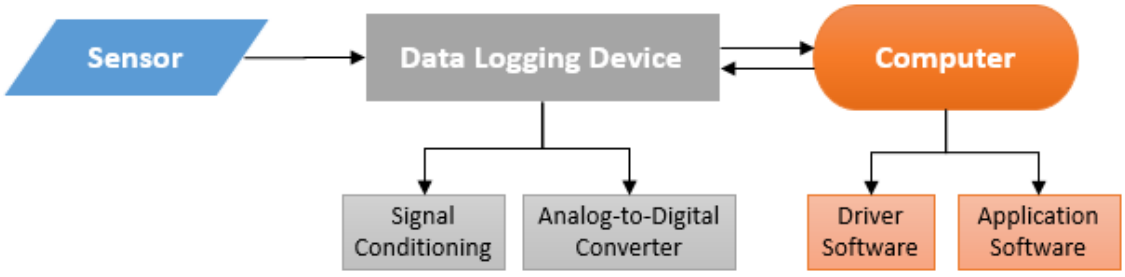

Figure 2.1: Schematic of a data logging system

2.1 System Design

AHU is studied by identifying the physical parameters/data needed to be collected to establish and perform FDD analysis. Robust and appropriate sensors are selected and installed to the AHU. And for the application, cloud-based devices are used, connecting and transferring data via internet signals. After the installation of the devices, operating data are collected, analyzed, and verified.

2.1.1 Mechanical System (Air Handling Unit)

In Figure 2.2 shows the simple schematic of the AHU investigated in this project. The system can be separated into four major components: outdoor climate, outside air intake, heat exchanger, and fan. Outdoor climate pertains to the seasons and weather

changes, latitude, longitude, and altitude of the building system. The outside air enters the system with the effect of the outdoor climate. Outside air intake refers to the mixing box dampers such as the exhaust/return air and outside air dampers which conserves energy and eliminates contaminants, particulate matter, and CO_2. This economizer can also enable the use of "free air" which means outside air that is at similar air temperature as the supply air that does not require cooling or heating. Any air that is not at the set point supply air temperature needs heating and cooling coil which is the heat exchanger section of the system. This project is mostly concerned of cooling coils due to its high consumption of energy compared to the heating coil. And the fan draws the air into the system with a VFD system that can regulate the fan speed thus conserving the power consumed by the fan motor.

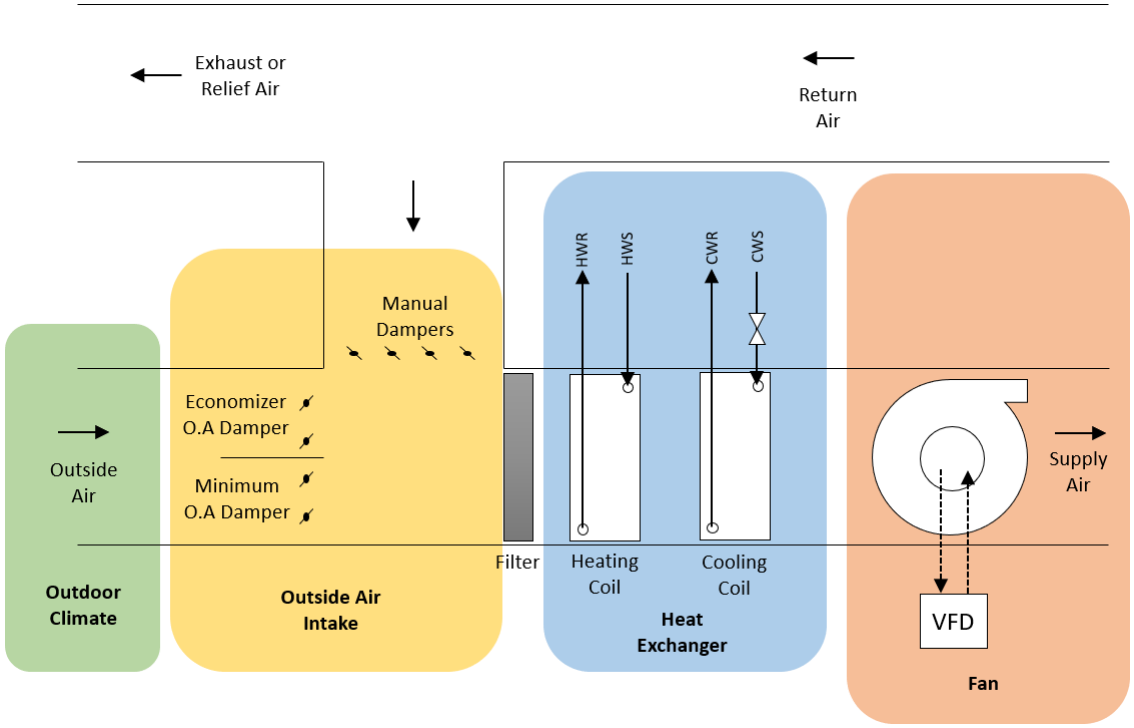

Figure 2.2: Air handler and associated components for specific VFD controlled system

2.1.2 **Design Criteria and Evaluation for Data Logging System**

The data logging system provides the access to data which is vital for collection of quality of the AHU performance, including the following four different categories of measurements per four major AHU components:

- Temperature and humidity of outside air
- Temperature of return air, mixed air, and supply air
- Cooling coil valve operation measurements including pressures and temperatures of inlet and exiting chiller water and voltage of valve actuator
- Supply air fan operation measurements including volumetric airflow of supply air, frequency and power of VFD control, and differential pressure of the supply fan.

Figure 2.3 shows the design installation locations of the sensors necessary to detect and collect data.

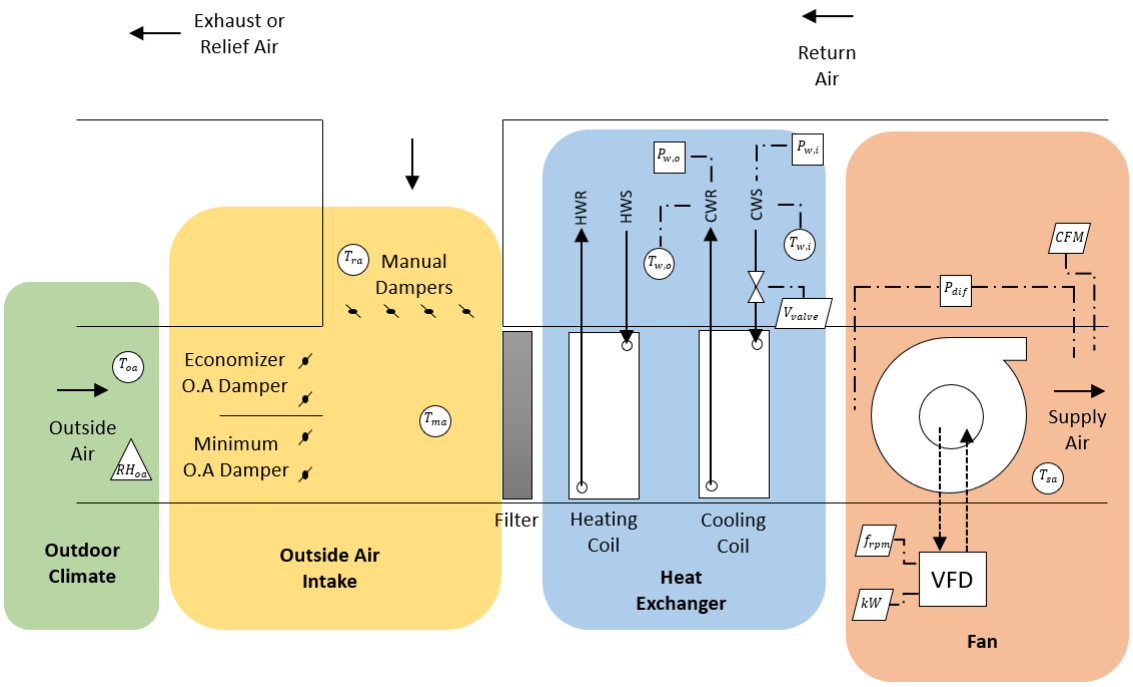

Figure 2.3: Measurement locations in air handling unit schematics

T_{oa}, T_{ra}, T_{ma}, and T_{sa} denote the measurements of temperatures of outside air, return air, mixed air, and supply air, respectively. RH_{oa} is relative humidity of the outside air. $T_{w,o}$ and $T_{w,i}$ are temperature of chiller water outlet and chiller water inlet, respectively. $P_{w,o}$ and $P_{w,i}$ define pressures of chiller water outlet and chiller water inlet, respectively. P_{diff} symbolizes differential pressure of the supply fan. V_{valve}, f_{rpm}, kW and Q denote, respectively, supply voltage to the actuator, frequency, or RPM, and power of the fan motor, and the volumetric airflow rate traveled through the unit.

2.1.3 Equipment Selection of Cloud-based Data Acquisition System

Paragon Robotics is a product manufacturing and cloud-service providing company with wireless data loggers and monitoring systems with remote wireless sensors. These sensors operate for applications such as energy efficiency auditing, building performance benchmarking, life sciences and vaccine monitoring, remote

property management, warehouse and storage monitoring and industrial process analytics. Paragon Robotics wireless data logging system is selected as traditional data logger system with features of real-time monitoring system.

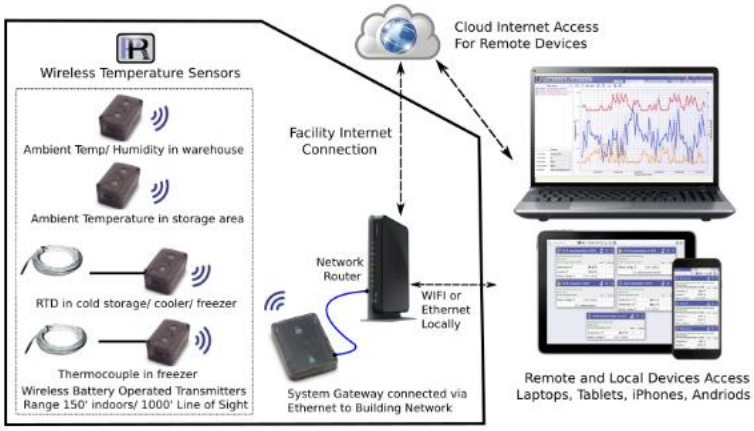

Figure 2.4: Diagram of Paragon Robotics Data Logging System Process

(source: http://paragonrobotics.com/)

Cloud Internet access, HaloCloud, is included as it provides remote access to the data logging system from any location via mobile device or PC with Internet connection. Paragon Robotics also provides widgets/tools in its website that can simultaneously connect for real-time data. Table 2.1 lists the equipment selected to the corresponding locations and uses.

Table 2.1: List of categories, devices, associated location and use

Categories	Tool/Device	Location	Use
Server	Gateway v4	Local Ethernet port	HaloCloud access and connectivity to sensors/devices
Outdoor Climate	SC12	T_{oa}, RH_{oa}	Measure temperature and humidity/log data

Outside air intake	Thermistor/SC31	T_{oa}, T_{ra}, T_{ma}, T_{sa}	Measure temperature/log data
Heat Exchanger	Thermocouple Probe/SC32	$T_{w,o}$, $T_{w,i}$	Measure temperature/log data
	200 psi pressure gauge/SC34	$P_{w,o}$, $P_{w,i}$	Measure pressure/log data
	0-5 V SC18	V_{valve}	Measure supply voltage/log data
Fan	4-20 mA & 0-5 V cable/TSI air velocity transducer/SC18	f_{rpm}, kW, Q	Measure output signals/log data

The **gateway** is required to simultaneously collect data from at least seven devices. It must store data into the cloud and capable of being access in any locations of the world. Other specific objectives of the gateway are it must be small and robust enough to be handled in other systems and easy to use for future projects. Gateway v4 is selected which features 32 GB of on-board memory for data storage and it provides interconnectivity for an unlimited number of devices at once. This gateway has connectivity range of 200 ft indoors. It has an Ethernet port that can be easily connected to any buildings with Internet access for the HaloCloud service.

Figure 2.5: Photo of the Paragon Robotics Gateway v4

The **thermistor** is needed to record the air temperature of outside air, return air, mixed air, and supply air. The air temperature fluctuates from approximately 0°F to 100°F. Therefore, an operating temperature range of the thermistor must be at least 0°F to 100°F. Finally, the accuracy of the device should be no more than 0.9°F of the readings. TR10-48M 10k metal probe thermistor is selected with the feature of temperature range of -40 ~ 175°F. SC 31 which has two inputs to attach two individual probes. The thermistors are shipped with 1200 mm (48”), so the length is extended to 15’ long with 24 AWG copper wires. Additionally, it is highly recommended to have humidity data points on all the mixed air, return air, and supply air, however not applications can allow perfect scenario. For this, **SC 12** device measures the outside air humidity and temperature to validate the outside air temperature carried into the unit.

Figure 2.6: Photo of the Paragon Robotics SC31 thermistor sensor with corresponding 10K thermistor, and SC12 temperature & humidity sensor

The water pressure is from around 20 psi to 60 psi. Since the sensor is measuring water pressure, the sensor must be robust and suitable. **Water pressure gauge** must be easily connectable to the chiller pipes. PX 309-200GV from Omega has a gauge pressure range from 0 to 200si. It is protected by an oil-filled stainless-steel diaphragm that is robust for the application. The pressure transducer has a 5VDC excitation and output of 0-100 mV output. 3.3 VDC provided by the SC34, a wireless bridge transducer and small signal sensor, affects the result of the mV output signal, so the calibration must be adjusted appropriately or supply the sensor with an external voltage of 5VDC. SC34 has data storage of 120 billion points with a transmission of low voltage signals from transducers and sensors. One device attaches to one transducer.

Figure 2.7: Photo of the Paragon Robotics SC34 bridge transducer and small signal sensor with Omega PX 309-200GV 200 psi pressure sensor

Thermocouple – type K and SC32 device are chosen for the measurement of liquid temperature. Thermocouple with a metal encapsulated tip has the range of -40°F to 1562°F. SC32 wireless sensor accepts thermocouple probe with a standard 2-pin flat connector including the type K. The metal needle tip is utilized to poke through the insulation of the chiller water pipe to detect the temperature accurately.

Figure 2.8: Photo of the Paragon Robotics SC32 thermocouple sensor with type K thermocouple

Differential pressure, airflow rate, VFD frequency and power are necessary to be recorded to analyze the supply fan performance. To identify and record the measurement of differential pressure, SC76 differential pressure sensor monitors the pressure between two air spaces. The fittings on the case can measure ± 1 psi (or 6.9 kPA) differential pressure with weather-resistant EPDM rubber tubing with 3/32" ID

and 7/32" OD. SC 18 external jack sensor accepts 4 external sensors including current measurements, air pressure, moisture, temperature, humidity, 4-20 mA, VDC, and more. SC18 device with the CST5 input cables is directed connected to TSI air velocity transducer, which can provide output signals of VDC or mA with maximum velocity of 4000 ft/s, and the VFD control panel to measure the velocity of air passing across the unit and the power/speed of the fan. SC18 is also utilized to measure and record the actuator valve movement of the chiller water cooling coil.

Figure 2.9: Photos of the Paragon Robotics SC76 differential pressure sensor, TSI Air Velocity Transducer, and SC18 external jack sensor with CST5 input cable (0-5V)

2.2 Installation/Validation

The cloud-based data logging system must be set up correctly to have effective results. This section explains a walk-through of how Paragon Robotics devices were installed into the AHU system.

2.2.1 **Gateway Claim/Connection**

A gateway is the device that enables the communication of signals between the sensors and a computer. It is required to tap into the calibration and logging settings of the sensors and to collect any data. Two types of gateways are recommended from Paragon Robotics which are Gateway v4 and Super Gateway v10. The Gateway v4 allows a wide distance of range of connecting to the sensors and storage capability of 120 billion data points with unlimited connections to the sensors. On the other hand, Super Gateway v10 is specifically designed to communicate with BACnet, Modbus or other custom network-based protocols. The gateway gives a much smaller range of sight and less amount of storage than Gateway v4. For this project, Gateway v4 is proven to be the better choice.

First, an account is registered in paragonrobotics.com website to gain access to the HaloCloud service, that Paragon Robotics provides, with an email and password. This can be found after clicking “Sign In” in the top right corner. Account credentials to access the project’s data is given to Dr. Li Song if needed to be studied.

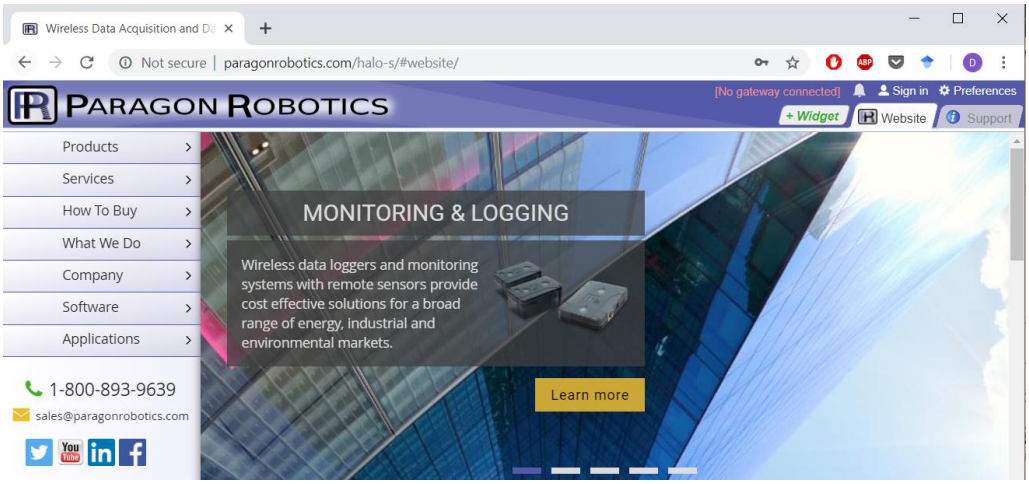

Figure 2.10: Paragon Robotics website (accessed in 3/22/19)

After registration, a widget tab of “SetupDevices” is created in the top-right corner to begin setting-up and connect the gateways and sensors. First, HaloCloud is set up properly as it is recommended to use HaloCloud and always sync the settings with HaloCloud. Then, the network security key is created with the email address and password.

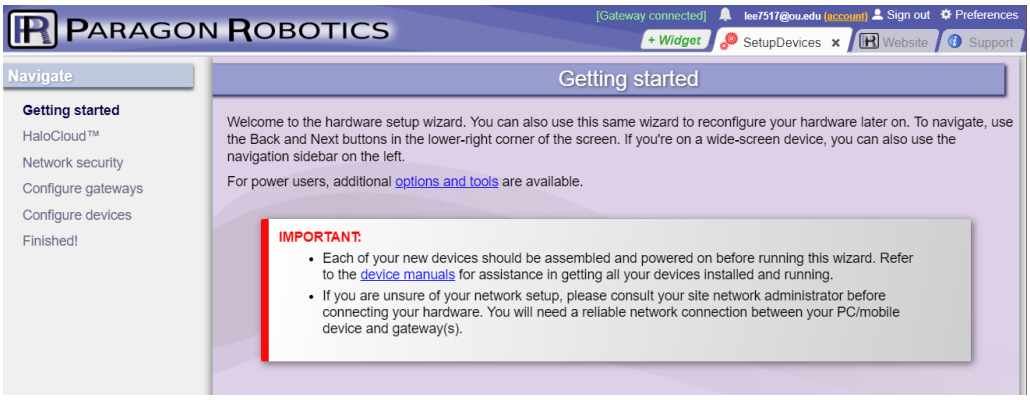

Figure 2.11: Getting started page in the “SetupDevices” tab (accessed in 3/22/19)

Depending on the type of internet connections, the procedure to configurate and connect the gateways is different. The gateways must be “Claimed” as the account’s device to access its data. And to claim the gateway, it must have Internet connection to communicate with the website. When the security level of internet is minimal, the gateway is capable of directly communicating after connected the Ethernet port. If the internet connection has high levels of security built-in like the University of Oklahoma that demands all electronic devices of internet access to be registered, the gateway must be claimed to the account before connecting it to internet. In this project, since OU was not able to directly connect the gateway to the internet with merely attaching the Ethernet cable to the operating port due to the incapability of registering the gateway itself (no keyboard and mouse connection), it was first claimed at a personal house with a less complex router, then transferred and connected to the Ethernet port (nearest to the

sensors to ensure good link to the output signals). If the gateway is claimed but outlined in the color of red instead of green, such as in Figure 2.12, check the gateways power or connection to the Ethernet port and call Paragon Robotics service team as it may not have power and/or internet connection, or the cloud server may be inoperative at the time for maintenance reasons.

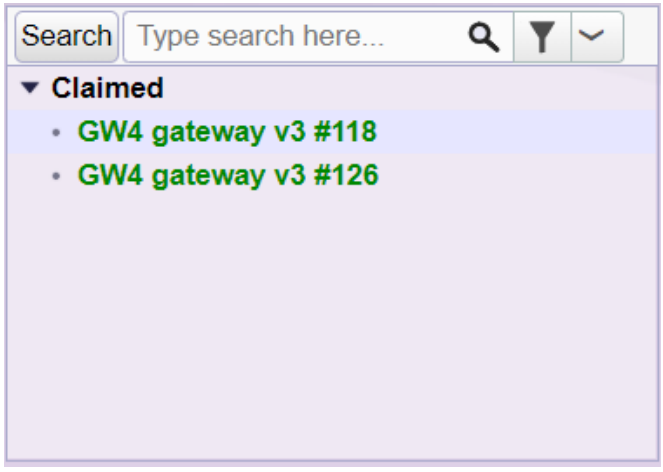

Figure 2.12: Example of properly claimed and connected gateway (accessed in 3/22/19)

When the gateways are connected to the ethernet ports, they must be in open area to ensure the best connection to the sensors with antennas facing upward and in clear of sight from furniture and such. The sensors cannot connect to the gateway inside metal enclosures, so the sensors must be selected appropriately to the application. Blinking of both LED lights in the physical Model of the gateway indicates good connections to power and internet as indicated in Figure 2.13.

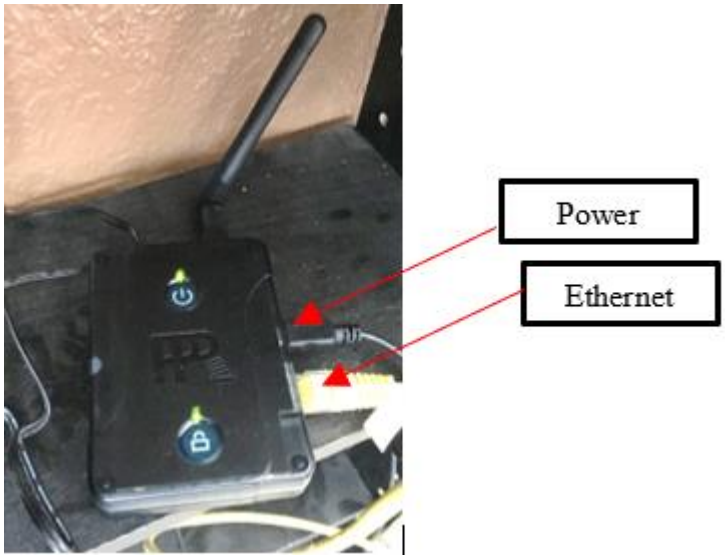

Figure 2.13: Picture of an operating gateway

2.2.2 Outdoor Climate

There are two types of units of humidity: absolute humidity and relative humidity. Absolute humidity is the mass of water vapor divided by the mass of dry air in a volume of air at a given temperature. Relative humidity is the ratio of the absolute humidity at the point to the maximum absolute humidity it can achieve in the temperature of that specific point. 100 percent of relative humidity means that the air is fully saturated. Absolute humidity can be calculated with three properties: pressure, or altitude, dry bulb temperature, and relative humidity.

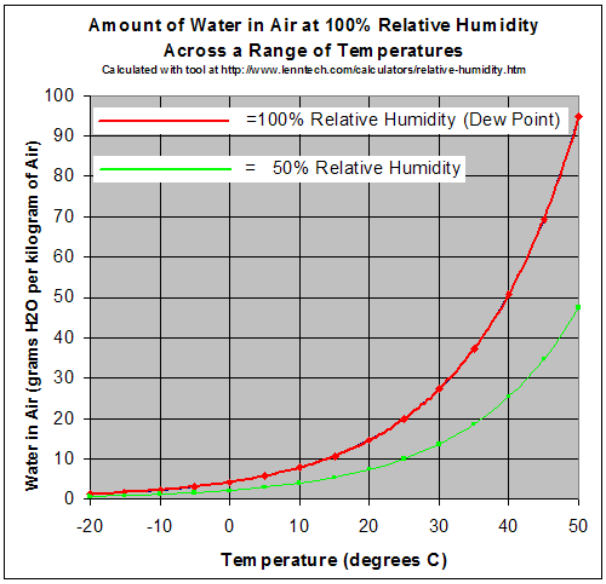

Figure 2.14: Relative humidity curve of 100% and 50% in range of -20°F and 50°F in respect to absolute humidity

Occupants are very sensitive to humidity, as the air removes moisture from human's skin and respiratory system. Sweating is the body's method of maintaining comfort and removing heat thus reducing the body's temperature. When the air is at 100 percent relative humidity, sweat cannot evaporate into the air. A high relative humidity (more than 60%) can reduce the evaporation process of the human body and encourage the growth of mold and mildew due to the moist and humid conditions. A lower relative humidity (less than 30%) can cause eye irritation, allergies, or spread of viral infections.

Humidity is an essential property to assess the quality of air. Air handling process not only cools the air but removes moisture for the human comfort in the buildings. ASHRAE guidelines recommend 68°F to 74°F in the winter and 72°F to 80°F in the summer and the relative humidity of 30% to 60%. The humidity is controlled mostly by using the level of humidity of outside air. Therefore, the relative humidity of the outside air is recorded and measured.

SC12 humidity sensor measures and records the temperature and the relative humidity. Due to the wireless signal communication problems when placed in metal enclosures, an outdoor enclosure was designed and manufactured with a plastic junction box and 3D printed louvers attached to the sides with an overhang structure to have well-ventilated air stream to detect the outside air precisely.

Figure 2.15: Photo of outside air temperature sensor case

The sensor is connected to the nearest gateway in the Configure Devices tab and placed inside the junction box. Using the DataAnalyzer widget tool, Figure 2.15 shows again a ± 0.9°F of error of SC12 device but accurately following the trend with the thermistor placed in the HVAC system measuring and recording the outside air temperature. The relative humidity measured by SC12 device is a function of the temperature reading from SC12. Therefore, when absolute humidity is to be measured, it must be converted by using an equation with the temperature data recorded from SC12, instead of any other temperature sensor or thermistor.

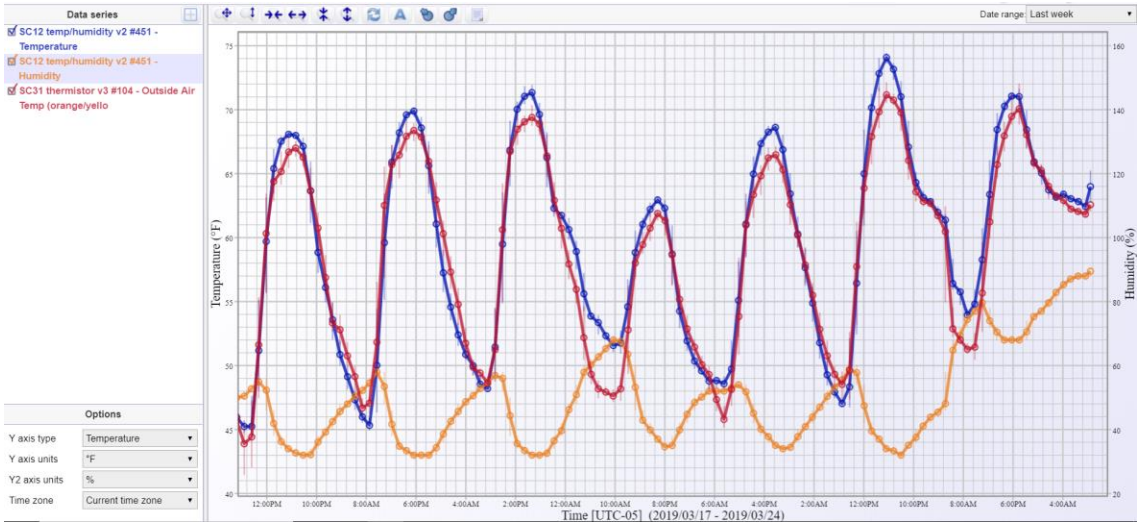

Figure 2.16: Data points of outside air temperature and humidity from SC12 wireless temperature/humidity sensor with outside air temperature from SC31 thermistor sensor over period of one week

2.2.3 **Outside air intake**

Thermistor is a component that changes resistance with temperature. This changing of resistance can translate to change in the voltage supplied and then converted into the temperature of the thermistor. One of the applications for a thermistor is to measure temperatures of the different types of air traveling through the AHU. In this project, two 10K thermistors, TR10-48M, are attached to SC31 device and two SC31 are used to record four air temperatures: return, mixed, outside and supply. The thermistors wires are extended by joining 15 ft 24 AWG copper wires. As indicated below, each thermistor has different colors of wires for labeling purposes to know where the data is collected from.

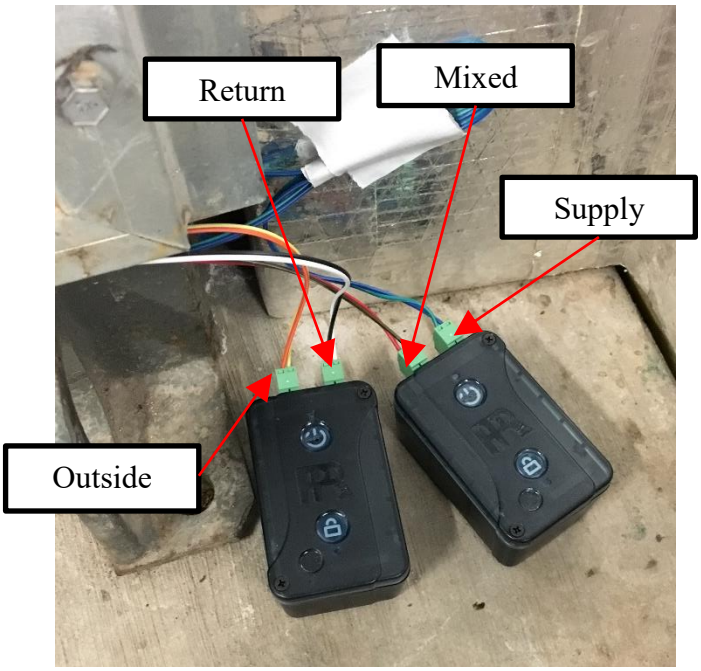

Figure 2.17: Two SC 31 devices with four connected thermistors and one thermistor set-up to detect mixed air temperature

The Paragon Robotics wireless sensors must all be claimed/connected to sync to the nearest gateway. In the “Configure devices” section of “SetupDevices” widget tab, When the devices are powered on (top LED next to the power button blinking), you can select the devices that are desired to be claimed and start communicating to the account. When the device cannot be seen, restarting the device may help to search the gateway again as it powers on. After it is claimed, a widget tab “DataRecorder” can be used to observe the output signals of the sensors, the connection bars, and the time it was synced as shown in Figure 2.18.

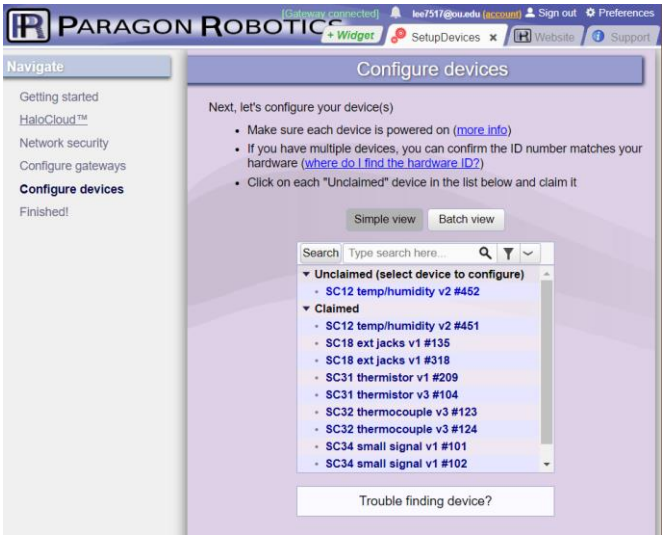

Figure 2.18: "Configure Devices" tab to claim or disclaim devices in the account

To verify that the thermistors are working correctly, these thermistors were placed in the same space location – Mechanical room where the AHU is placed in – with a SC12 temperature/humidity sensor for 48 hours. Widget tab of "DataAnalyzer" can show a graphical image by choosing which data series is desired to be observed. Figure 2.19 conveys the temperature of the room measured with the four thermistors and SC12. The thermistors are more reliable than SC12 in accurately measuring the temperature, thus any reading of the outside air comes from the thermistor detecting the outside air temperature. The thermistors have less than 0.5% error with each other confirming that all the thermistors are working properly with reliable data measuring and logging ability.

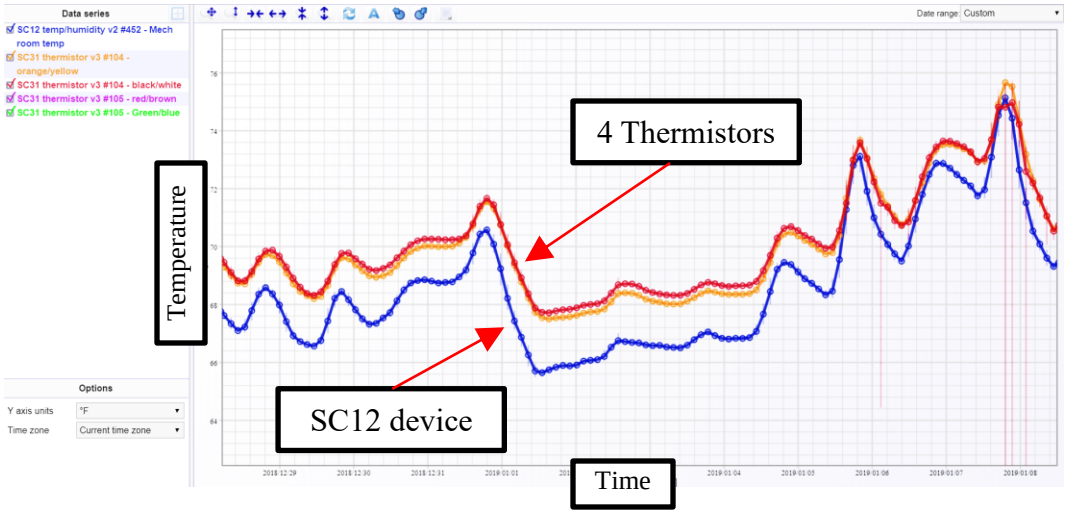

Figure 2.19: Paragon Robotics graphical interface of temperature change of mechanical room measured with 4 thermistors and SC12 temperature/humidity sensor (accessed in 3/23/19)

The four thermistors are then placed in each location: blue/green wired thermistor near the supply fan after the cooling coils, red/brown wired thermistor beside the filter after outside and return air is mixed, white/black wired thermistor behind the return air dampers, and orange/yellow wired thermistor behind the outside air damper.

SC31 thermistor v1 #209

OK (synced less than 1 minute ago)
Group: None
ID: SC31 thermistor v1 #209

		Alarm	Logging
Mixed Air Temp (red/brown)	63.8 °F	-	✓
Supply Air Temp (blue/green)	49.9 °F	-	✓
Battery voltage	2.83 V (85%)	-	-

SC31 thermistor v3 #104

OK (synced less than 1 minute ago)
Group: None
ID: SC31 thermistor v3 #104

		Alarm	Logging
Outside Air Temp (orange/yello	55.8 °F	-	✓
Room Air Temp (white/black)	71.2 °F	-	✓
Battery voltage	2.83 V (85%)	-	-

Figure 2.20: Real time software interface of the thermistors and SC31 devices (accessed in 3/23/19)

After logging a full recording of one week without any fault introduced to the system, the data can be exported and compounded into excel if necessary. Figure 2.21 shows a side-by-side comparison of the graphical profiles of the four thermistors from

Microsoft Excel and Paragon Robotics. This figure represents a good reading of the temperatures because the mixed air must always be between return air and outside air due to the mixing process in the unit.

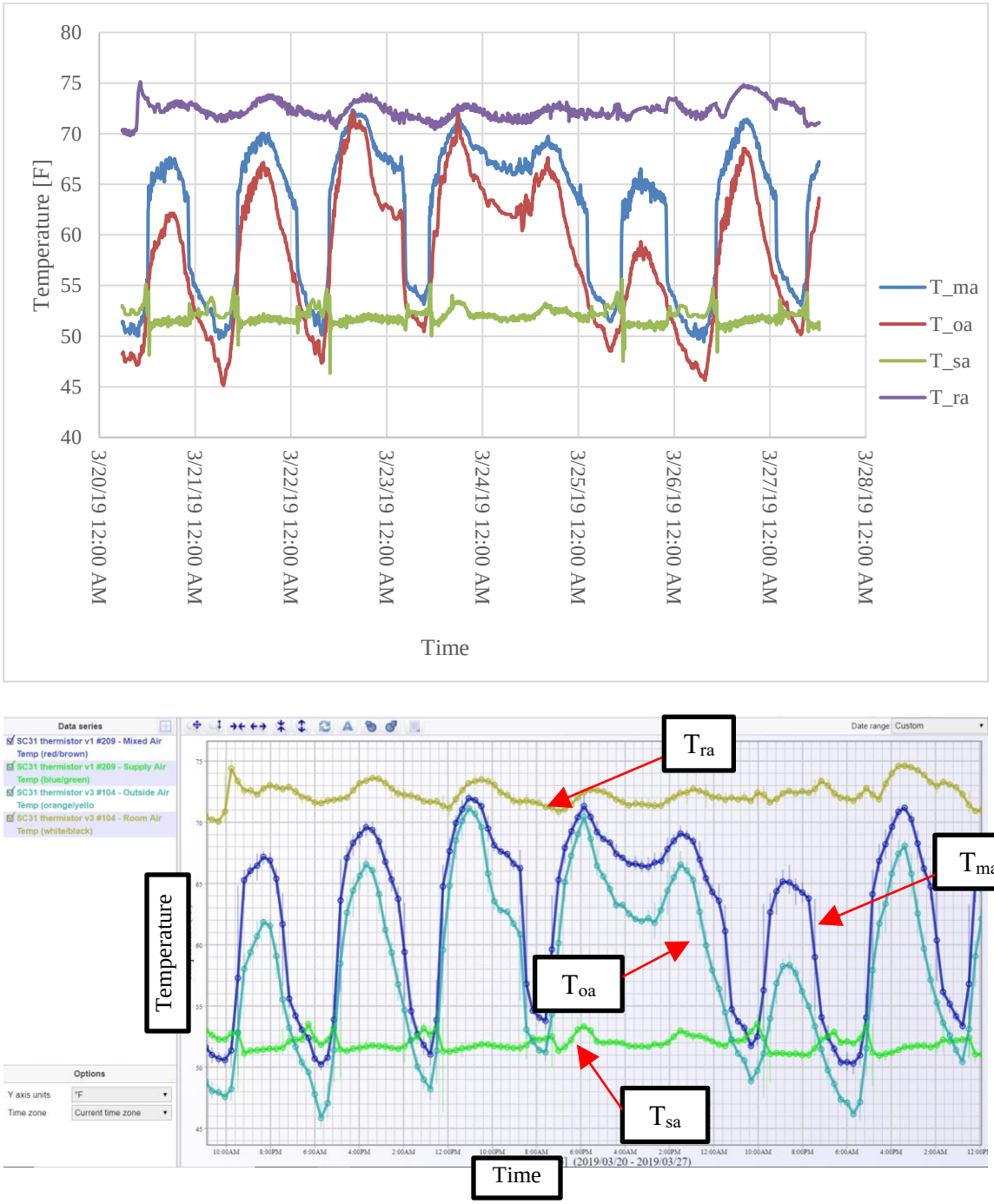

Figure 2.21: Temperature of outside air, mixed air, supply air, and return air in a period of one week represented through two different interfaces (accessed in 3/23/19)

Outside air intake has governing engineering principles of dry air mass balance (Equation 1), energy balance (Equation 2), latent heat balance (Equation 3), and sensible heat balance (Equation 4). Equation 5 is the definition of the enthalpy.

$$m_{oa} + m_{ra} = m_{ma} \tag{1}$$

$$m_{oa} i_{oa} + m_{ra} i_{ra} = m_{ma} i_{ma} \tag{2}$$

$$m_{oa} i_{latent,oa} + m_{ra} i_{latent,ra} = m_{ma} i_{latent,ma} \tag{3}$$

$$m_{oa} i_{sensible,oa} + m_{ra} i_{sensible,ra} = m_{ma} i_{sensible,ma} \tag{4}$$

$$i = c_p T + h_v W \tag{5}$$

where m is the mass, i is the enthalpy, c_p is the constant moist air specific heat of 0.242 $\frac{Btu}{lbma*°F}$, T is the temperature of the air, h_v is the constant vapor enthalpy of 1074 $\frac{Btu}{lbma}$, and W is the absolute humidity of the air. Sensible and latent heat are decoupled to further simplify the equations as shown in Equation 6-9.

$$\alpha = \frac{Q_{oa}}{Q_{oa}+Q_{ra}} \tag{6}$$

$$i_{oa} = \alpha * i_{oa} + (1 - \alpha) * i_{ra} \tag{7}$$

$$W_{ma} = \alpha * W_{oa} + (1 - \alpha) * W_{ra} \tag{8}$$

$$T_{ma} = \alpha * T_{oa} + (1 - \alpha) * T_{ra} \tag{9}$$

where α is the ratio of the outside air and the mixed air.

Airflow rate of outdoor air intake is difficult to measure. The alpha can be determined not only through the volumetric airflow rate but also with the temperature as shown in Equation 9. With the measurements from the data logging system, the alpha ratio can be calculated as shown in Figure 2.22.

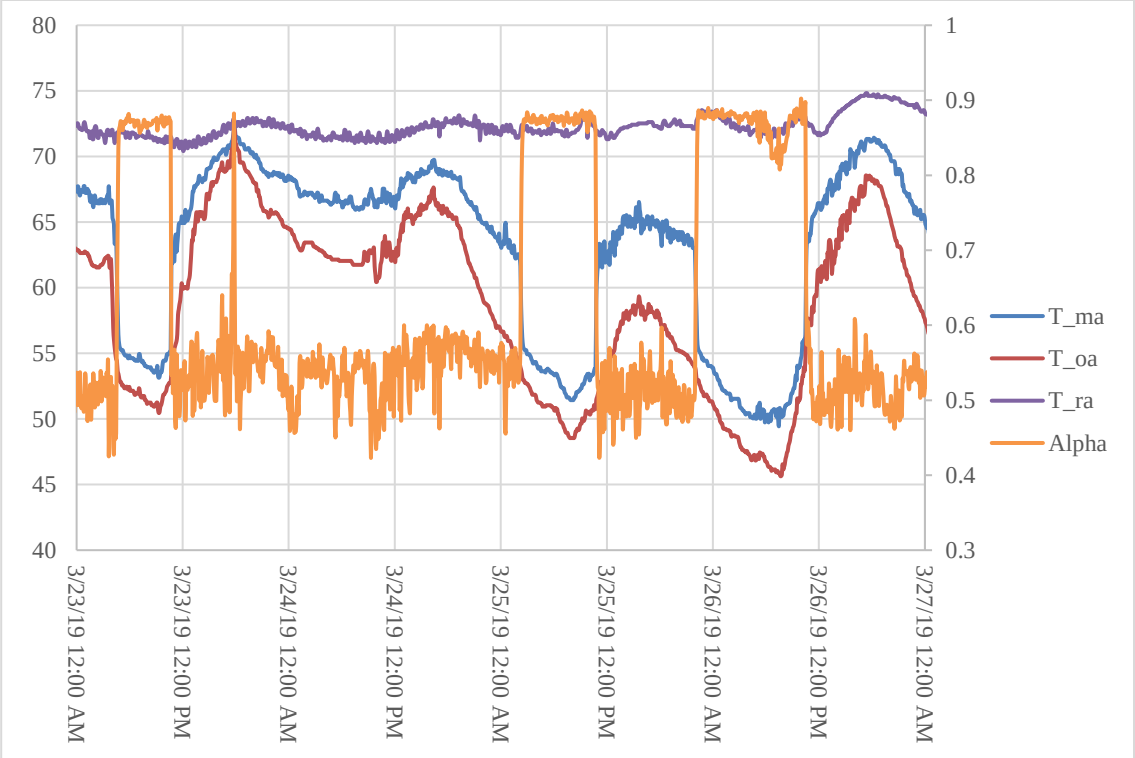

Figure 2.22: Alpha ratio with temperature of mixed air, outside air, and return air

The α is highest when the temperature of outside air is lower than or equal to 55°F, which is the supply air set temperature. This alpha ratio is used to determine the energy used to dehumidify the air in hot and humid outdoor air climate with Equation 8. The "free air" operation is meant to introduces 100% of outside air while return air damper is blocked to utilize the least mechanical cooling and save energy consumption. However, the measurements show the highest alpha ratio is less than 90%. This can be interpreted as the return air damper has leakage. Due to the higher temperature of the mixed air compared to the outside air temperature during the free air operation, the existing operation is not optimal or fault-free.

2.2.4 **Heat Exchanger**

The cooling coil is a key component of the AHU system as it is the primary way of cooling the air as the air is drawn through the coils by the fan. The amount of cooling is controlled by the actuator valve that can close and open to the necessary amount for its demand. The amount of energy needed to be cooled must be equal to the energy gained to satisfy the supply air temperature requirement. During mechanical cooling, AHU uses the actuator valve positioning control to control the flow and pressure of the cooling coil. The exiting and entering temperature of the cooling coil is essential to analyze the effectiveness of the energy transfer of the cooling coil.

The **type K thermocouple** probe with a metal penetrating probe is attached to the SC32 device. The thermocouples penetrate through the insulation to touch the cooling coil pipe to ensure accurate reading of the temperature. The SC32 device is then claimed and connected as any other devices in the “Configure device” tab shown in Figure 2.15. SC18 is used with an input cable of 0-10 VDC to detect the positioning of the actuator valve of the chiller water. The cable is installed into the actuator valve connect to receive output signal of VDC to identify the positioning of the actuator valve.

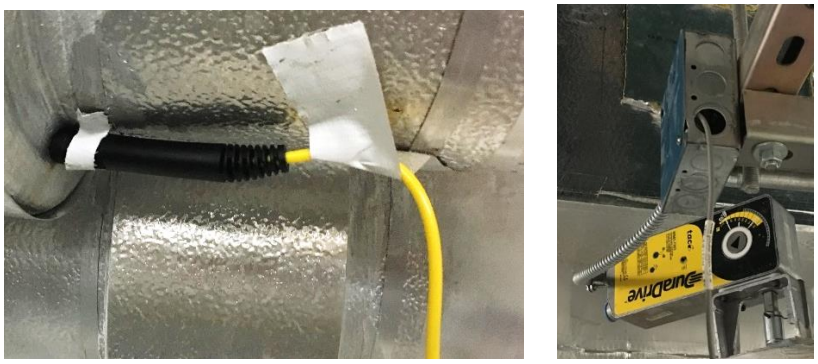

Figure 2.23: Type K thermocouple installed and penetrated through the insulation and 0-10 VDC cable installed to actuator valve of chiller water pipe

Figure 2.24 depicts the graphical image of the position of the valve and the cooling coil energy transfer. As the valve increases in voltage, inversely, the chiller

water inlet and outlet temperature decrease. And as the valve decreases in voltage, the chiller water inlet and outlet temperature increase. Decrease voltage means a more opened position of the valve and increased voltage indicates a more closed position to stop the energy transfer. It infers that when cooling load is less (during night time), the valve actuator closes the flow of the chiller water and when the cooling load increases, the valve actuator opens to provide the cooling phenomenon. The DuraDrive linear actuator valve is controlled with proportional Models by 2-10 Vdc signals and set in a direct-action function (output signal increases as valve opens, or flow rate increases). It has a dial feature that can control the maximum percentage of opening of the valve. It is set to 60%, depicted in Figure 2.23.

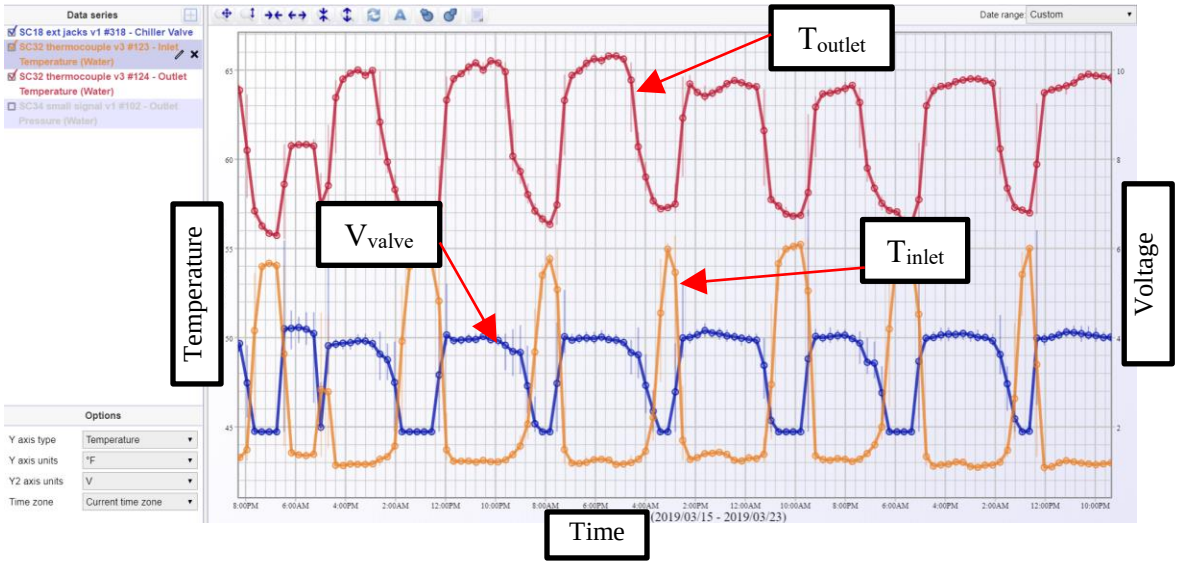

Figure 2.24: Relationship between chiller water inlet and outlet temperature and actuator valve output signal during a week period (accessed 3/24/19)

The heat transfer process can be examined with the fundamental principle of conservation of energy. The total energy transferred from the air to the chiller water coils in the cooling coil section must be equal. The energy transferred can be categorized as sensible or latent heat. Sensible heat is associated with the heat related to

the temperature change. Latent heat involves the heat caused by phase change of a compound. In the AHU, the evaporator coils, chiller water coils in this case, has features of cooling of air temperature and dehumidification. So, when the outside air is dry, such as in the spring season (the testing season for the thesis study), the total energy can be represented by the sensible heat from the cooling of air temperature, which must be equal to the logarithmic mean temperature difference (LMTD). LMTD is used to determine the temperature driving force for heat transfer in flow systems.

$$\dot{q}_{air-side} = \dot{q}_{water-side} = \dot{q}_{\log mean\ temperature\ difference} \tag{10}$$

$$q_{air-side} = q_{sensible} + q_{latent} \tag{11}$$

$$q_{\log mean\ temperature\ difference} = U * A * LMTD \tag{12}$$

$$q_{sensible} + q_{latent} = U * A * LMTD_{cross-flow} \tag{13}$$

where as $\dot{q}_{air-side}$ denotes the air-side heat transfer rate, $\dot{q}_{water-side}$ is the water-side heat transfer rate, $\dot{q}_{\log mean\ temperature\ difference}$ is the heat transfer rate of the cooling coils expressed with log mean temperature difference method, $q_{sensible}$ is the sensible heat, q_{latent} is the latent heat, U is the heat transfer coefficient, A is the exchange area, and $LMTD$ is defined as logarithmic mean.

The logarithmic mean temperature difference is defined differently in two applications: cross-flow or parallel flow. In this application, the airflow through the cooling coils are considered as cross-flow, and the air is considered as hot fluid and the chiller water as cold fluid in Equation 14.

$$LMTD_{cross-flow} = \frac{(T_{hot,inlet} - T_{cold,inlet}) - (T_{hot,outlet} - T_{cold,outlet})}{\ln(\frac{(T_{hot,inlet} - T_{cold,inlet})}{(T_{hot,outlet} - T_{cold,outlet})})} \tag{14}$$

$q_{sensible}$ is defined as the product of the air temperature difference of the inlet and outlet, volumetric airflow rate, specific heat of air, and density of air. The $U * A$ and $c_p * \rho$ in Equation 15 is considered constant which only affects linearly and q_{latent} is assumed as zero, thus Equation 15 is formed and used to verify the data measured with the thermistor and temperature probes.

$$q_{sensible} = c_p * \rho * Q * \Delta T = UA * LMTD_{cross-flow} \quad (15)$$

$$C * Q * \Delta T = LMTD_{cross-flow} \quad (16)$$

where C represents a constant value.

Figure 2.25 shows the relationship between the product of air-side temperature difference and volumetric flow rate and the LMTD. This demonstrates the quality of the measurements from the sensors.

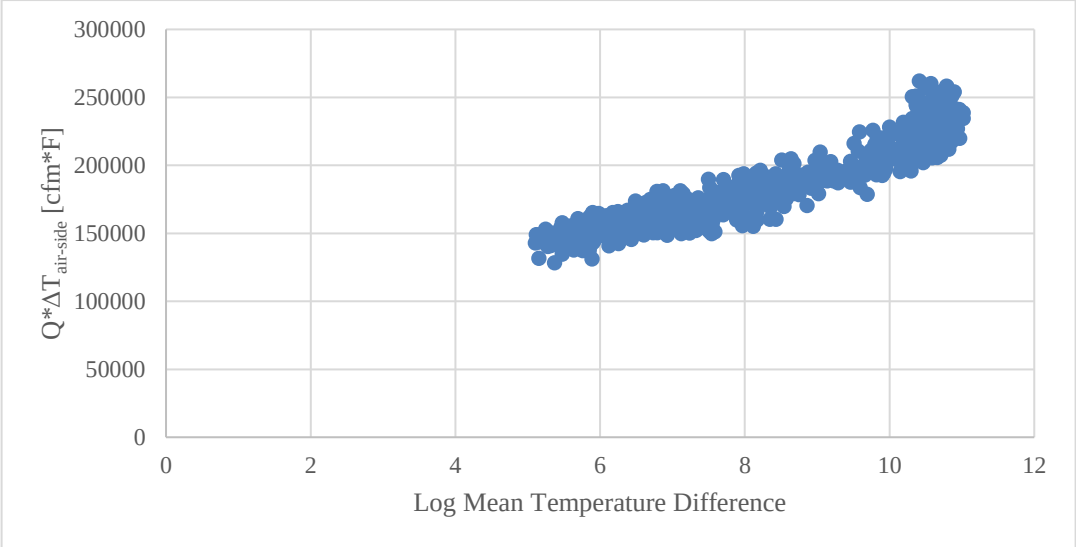

Figure 2.25: Relationship of the product of volumetric flow rate and temperature difference of mixed air and supply air and the log mean temperature difference (accessed 4/8/19)

Figure 2.26 shows the representation of the water-side temperature difference and the log mean temperature difference, but due to the transient response of the valve

and the cooling effect, the graph does not show a well-defined linear pattern. Also, the valve position signal was very constant of 0% and 40% not providing enough data in between those positions.

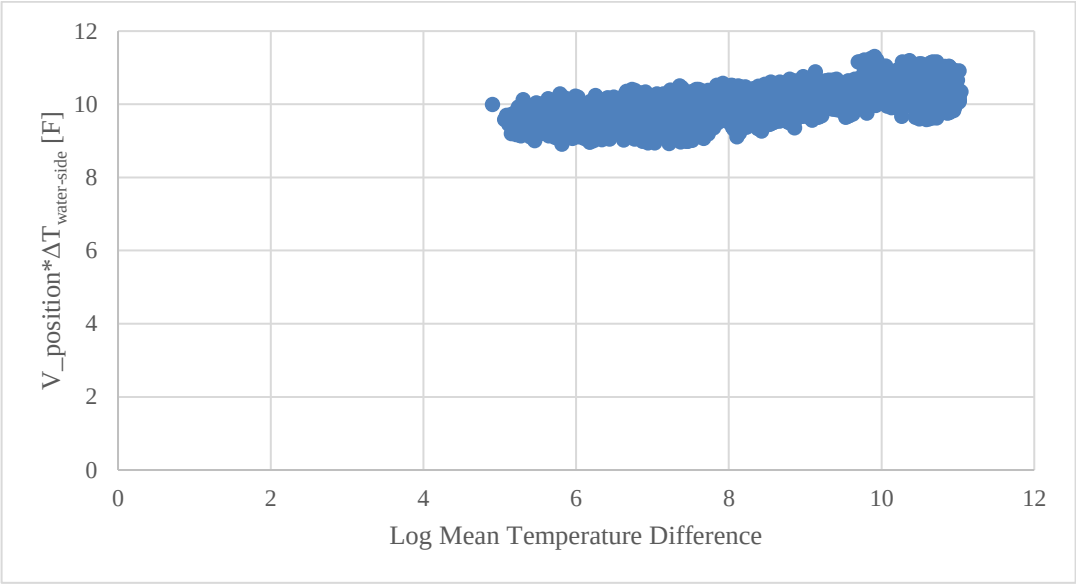

Figure 2.26: Relationship of the product of the position of the valve and temperature difference of chiller water inlet and outlet and the log mean temperature difference (accessed 4/8/19)

Figure 2.27 shows the installation of the pressure sensor. A pressure gauge with a meter that displays the pressure reading at that time is connected to calibrate the Paragon Robotics device. Omega PX309-200GV is a pressure gauge that has an input voltage of 5 VDC and outputs signal voltage range of 0-100mV corresponding to the measurement of pressure range from 0 to 200 psi. The issue of the Paragon Robotics device that reads the output mV readings from the pressure gauge could only generate 3 VDC for the Omega sensor, creating the output signal to skew. The calibration did not work as needed to, so an external power supply was added to provide the 5VDC to the gauge.

After verification of the output signal to give the right amount of mV with a multimeter, the output signal wires were connected back to the device. However, it was later discovered that the device is hardwired with a specific calibration system and it could not read the output signal with 5VDC powered sensor. Although pressure measurements of the chiller water would have been extremely useful examine the performance of the water flow versus the position of the valve, but due to the time constraints of the project, it is no longer investigated with priority.

Figure 2.27: Chiller water pressure gauge installation with the Paragon Robotics device to detect the mV output signal from the Omega pressure gauge

2.2.5 Fan

Flow of any fluid is caused by difference in pressure between two points. The direction of that flow equals high pressure to low pressure, or high energy to low energy. In HVAC systems, fan head pressure causes the flow to occur. Flow of air in duct is defined by three fundamental laws of physics: conservation of mass, conservation of energy, and conservation of momentum.

Bernoulli's equation (Equation 17) uses the conservation of mass and conservation of energy in terms of pressure in a flow with two points.

$$P_1 + \frac{\rho {v_1}^2}{2} + \rho g z_1 + \rho w = P_2 + \frac{\rho {v_2}^2}{2} + \rho g z_2 + \rho g \Delta l \quad (17)$$

where P is pressure at certain point, ρ is density, v denotes velocity, g is the gravitational constant, z is the height of the certain point, w/ ρ is the fan or pump pressure head, and l is the distance of the pressure loss. And for air fan, Bernoulli's equation can be condensed down to Equation 18. When this equation is simplified by the assumption of the fan inlet total pressure reflects the total pressure lost upstream of the fan and the fan outlet total pressure reflects the total pressure lost downstream of the fan, Equation 19 is formulated. Fan head, or the differential pressure of the fan, is very essential for the AHU operation as it provides the flow of the whole system.

$$P_{o,1} + \rho w = P_{o,2} + \rho g \Delta l \quad (18)$$

$$\Delta P_{fan} = \rho g H_{fan} = \rho w = P_{0,outlet} - P_{0,inlet} = \sum (\Delta P_{0,i})_{up} + \sum (\Delta P_{0,i})_{down} = \sum \Delta P_{0,i} \quad (19)$$

Differential pressure sensor is installed to measure the fan head pressure. The tubes connect to the device and the other ends of the tubes are placed before the fan and after the fan. Figure 2.28 is a visual representation of how the tubes are placed in specific locations to sense the static pressure. The pressure is translated to inch.water and this measurement is utilized to assess the performance of the fan compared to the fan curve given by the manufacturer. Figure 2.29 gives the graphical interface of the differential pressure in real-time through the Paragon Robotics "DataAnalyzer".

Figure 2.28: SC76 Differential Pressure sensor with two tubes connected. One tube connected to the duct after supply fan into tee tube fitting for negative pressure reading

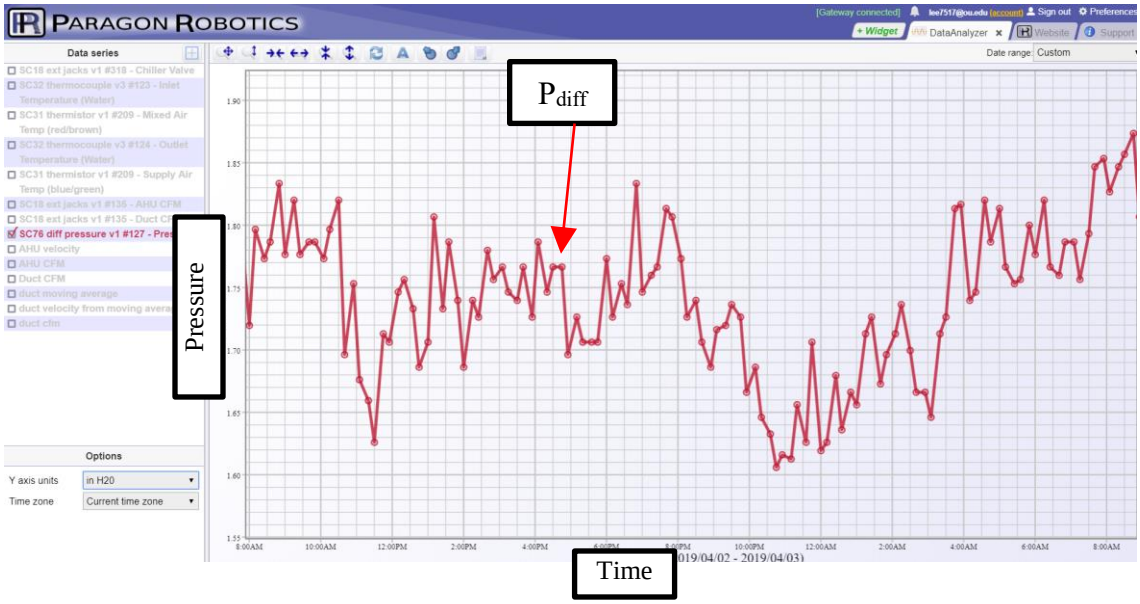

Figure 2.29: Differential pressure measured in inch.water (accessed in 4/3/19)

Conservation of mass states that mass is neither created nor destroyed. The mass of air coming into a specific volume in the HVAC system is equal to the mass of air leaving. And because air is assumed to be incompressible in HVAC systems, the change of air density is zero. This can be translated into the equation of volumetric air flow exiting is equal to the volumetric air flow entering. That volumetric air flow rate can be separated to the product of velocity of the flow and area. This introduces Equation 20.

$$v_2 = \frac{(v_1 * A_1)}{A_2} \tag{20}$$

where, v is velocity and A is area. In AHU system, this equation can be used to determine the new air velocity with the new cross-sectional area size.

Two TSI air velocity transducers are installed in different points throughout the AHU system, one in the duct right after the fan supply and the other in the AHU before the cooling coil system. The opening in the tip of the probe is carefully placed to be horizontal against the flow to allow most accurate reading. The data recorded from the probe in the ductwork is reviewed with caution due to the turbulence created by the bend of the ductwork.

Figure 2.30: TSI air velocity transducer installed in supply ductwork

The velocity probes calculate the velocity, and the output signal is given in the units of mA. The range of the output signal is 4-20 mA and the range of the velocity that the probe can measure is 0-4000 ft/min. This gives the linear relationship of Equation 21.

$$v\left[\frac{ft}{min}\right] = \frac{4000}{16} * \left(A_{cfm}\,[mA] - 4\right) \tag{21}$$

where, A_{cfm} is the output signal from the transducer in mA units.

Although the airflow velocity measurements of the probe in the duct is unreliable, the data can be used to see if it has similar range of volumetric airflow rate as recorded with the probe. The velocity measurements in, ft/min, are converted to

volumetric airflow rate, in units of CFM, by multiplying the cross-sectional area of the flow. Cross-sectional areas of the duct and AHU are 24 and 60 ft^2, respectively. Meanwhile, simple moving average equation, in Equation 22, is used to reduce and filter the noise of the signal of the duct velocity probe.

$$\bar{p}_{sm} = \frac{p_M + p_{M-1} + \cdots + p_{M-(n-1)}}{n} = \frac{1}{n}\sum_{i=0}^{n-1}(p_{M-i}) \quad (22)$$

Figure 2.31 shows the airflow rate detected in AHU and the supply duct. Although the volumetric flow rate is in a similar range, the duct measurement modulates too heavily even with the simple moving average filter applied (5 samples). This volumetric airflow rate points of the AHU are utilized in the later sections to determine the operating conditions of the supply fan.

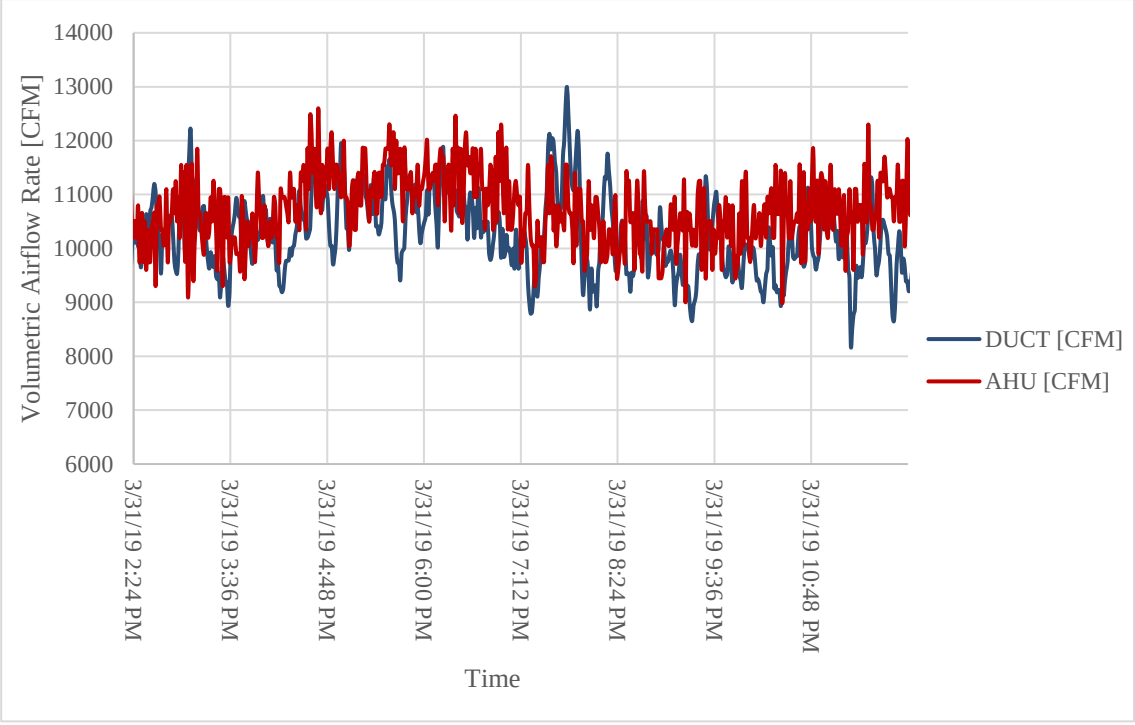

Figure 2.31: Volumetric airflow rate measured and recorded in supply duct and AHU during 12 hours (accessed in 4/1/19)

VFD control systems are widely used in fans, pumps, and compressors in HVAC systems, and in this application, VFD control system is used for the fan motor control to modulate the speed and maintain the discharge air static pressure or the temperature in worst zone at its set point. Compared to a VAV system of controlling the supply airflow rate to the spaces with damper modulation, VFD system, by adjusting the fan speed which directly translates to level of power consumption of fan motor, is expected to have maximum potential energy savings of 75%. VFD can also measure several useful electrical-related parameters, which could be used for system monitoring and FDD purposes.

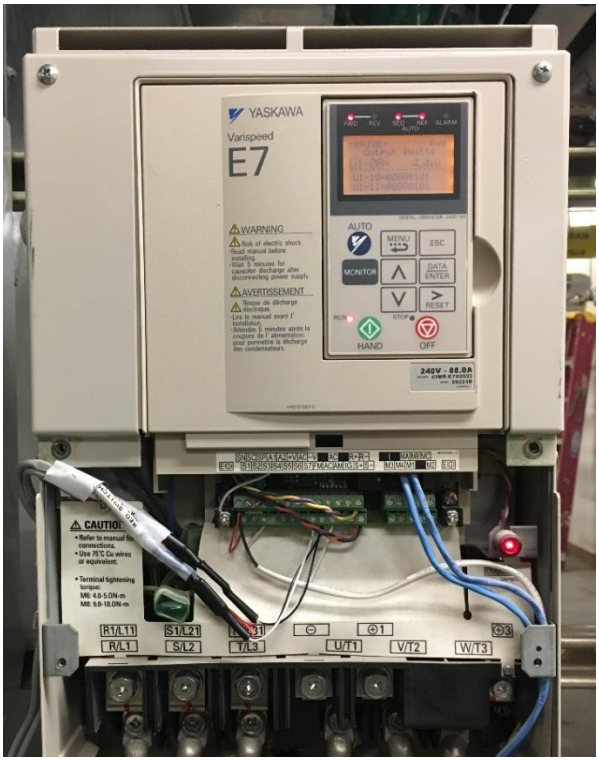

Figure 2.32: VFD control panel with 0-10 VDC wires connected

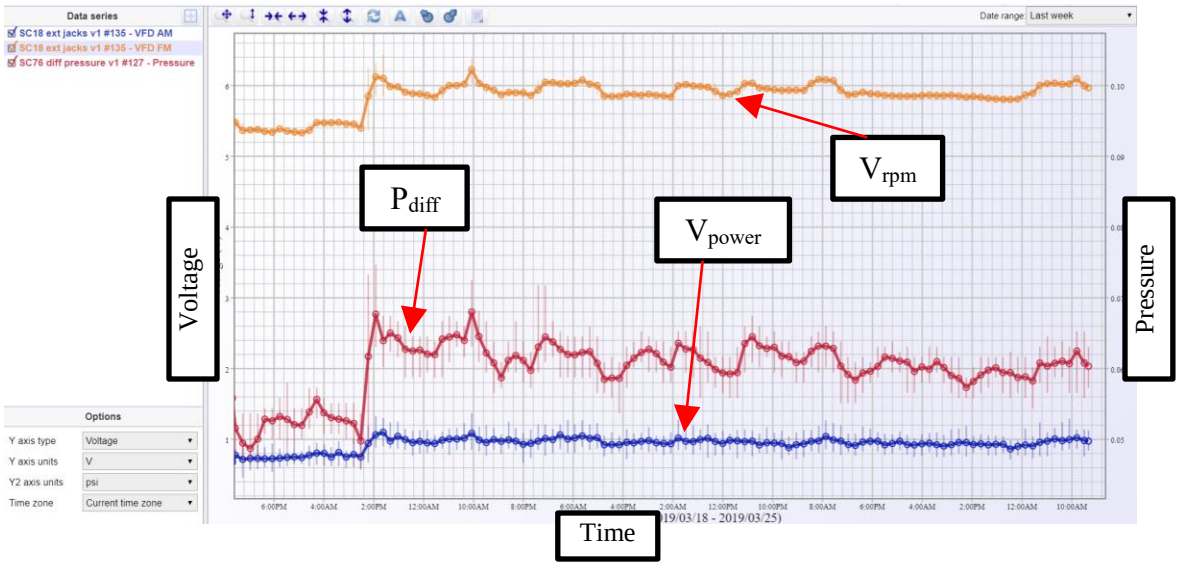

Figure 2.33: Relationship of fan speed and power output signals of VFD in V and differential pressure in inch.water

Figure 2.32 shows the VFD system panel and the output signal wires connect so the data logging system can record it. And Figure 2.33 depicts the relationship between rpm and power output signal in voltage, verifying that data logging system is correctly connected because rpm and power are both increasing and decreasing simultaneously. By obtaining the maximum fan speed in rpm and power in horsepower in the Fan Schedule from the AHU design specification (Appendix A), the output signals of fan speed and power can be converted with Equation 23 and 24.

$$Fan\ speed\ [rpm] = 138.1 * V_{rpm}\ [V] \tag{23}$$

$$Power\ [kW] = (V_{power}\ [V] * 2 * 30 * 0.746) \tag{24}$$

where, V_{rpm} is output signal of AM and V_{power} is output signal of FM.

In HVAC system, the relationship of the airflow rate and the pressure of the system is expressed as second polynomial increasing function in Equation 25.

$$H_{fan} = \Delta P_0 = SQ^2 \tag{25}$$

where S is the system resistance factor, which depends of the duct size and damper position. From this equation, this system characteristics curve is drawn and compared with the curve given in the submittals by the manufacturer, Nortek. This equation then introduces the Fan Law (Equation 26-28) giving the relationship of the airflow and fan speed (Fan Law 1), fan head and fan speed (Fan Law 2), and fan power and fan speed (Fan Law 3).

$$\frac{Q}{Q_{known}} = \frac{\omega}{\omega_{known}} \tag{26}$$

$$\frac{H}{H_{known}} = \left(\frac{\omega}{\omega_{known}}\right)^2 \tag{27}$$

$$\frac{P}{P_{known}} = \left(\frac{\omega}{\omega_{known}}\right)^3 \tag{28}$$

Appendix B is the AHU data sheet from the submittal of the manufacturer. In page 2 of the data sheet, a fan curve of rpm 1381 is given with its system curve. This fan curve and system curve is recreated in Figure 2.34. This figure also shows the fan head and its corresponding CFM (CFM data is of the velocity probe in the AHU). The fan head and CFM is then corrected by using Equation 28, 29, and 30 adjusting the speed to 1381 RPM which are derived from the Fan Law and is plotted in the figure to compare with the curves provided by the manufacturer.

$$H_{fan,d} = \frac{H_{fan,measured}}{\left(\frac{\omega_{measured}}{\omega_d}\right)^2} \tag{28}$$

$$Q_d = \frac{Q_{measured}}{\left(\frac{\omega_{measured}}{\omega_d}\right)} \tag{29}$$

$$P_d = \frac{P_{measured}}{\left(\frac{\omega_{measured}}{\omega_d}\right)^3} \tag{30}$$

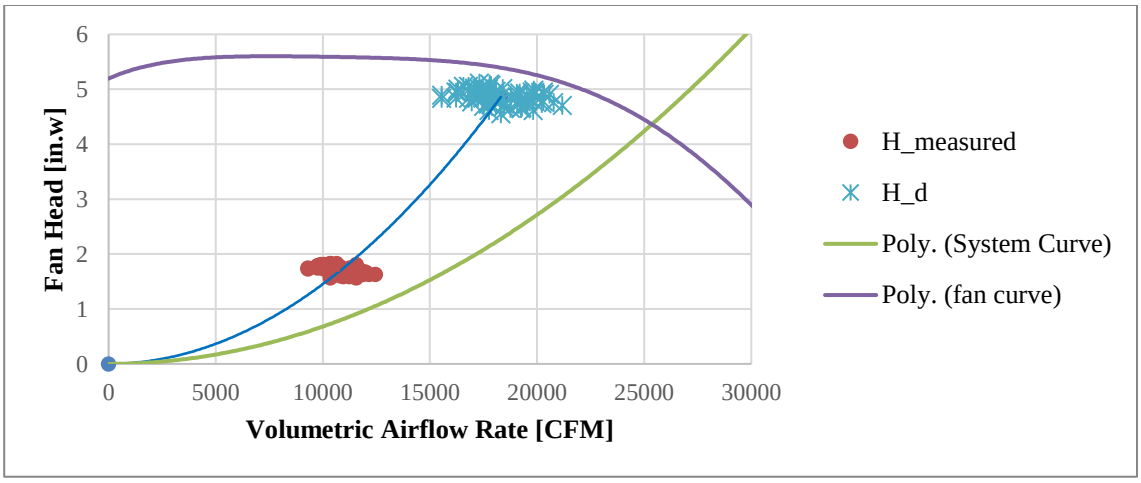

Figure 2.34: Fan head vs airflow rate and power vs airflow rate with fan curve from the manufacturer

As shown in the figure, depending on the outdoor climate, the fan head and volumetric can change. Thus, the longer range of data collection result in a wider range of the system curve. The baseline system curve (blue curve) compared to the system curve form the manufacturer shows that the system is already operating in a higher S curve indicating that there is a greater fan head, or total static pressure, with a lower volumetric flowrate. With the greater S value, the fan consumes more power to achieve the same amount of fan total static pressure.

2.3 Conclusion

After examination of the AHU system, the data logging system is selected to appropriately detect the necessary variables to study the AHU performance. Paragon Robotics devices are installed accordingly and calibrated to record accurate measurements. Then, the devices underwent an experiment of one to two weeks to observe the current state of each section of AHU and analyzed.

Chapter 3: FDD Development

As mentioned in the introduction, FDD analysis has different categories of methods. FDD methods range from those based on physical and analytical Models to those driven by analysis of historical performance data using either artificial intelligence or statistical techniques. The method of FDD applied to a system differs depending on the following:

- The type of system to which it is applied
- The level of detail of diagnosis required
- The cost of implementation
- The degree of automation
- Tolerance of false positives
- The quantity of input data required
- The number and location of sensors present

Although development of methods using combination of different techniques has been popular and effective, a simple rule-based method is chosen to be the most optimal decision to determine the next step of analytical FDD methods with the cloud-based data logging system. The rule-based method is dependent on type of fault that is examined, thus the common faults of AHU systems are identified, and the method is developed to detect the specific faults observed from the list. In this chapter, the development of FDD method is described.

3.1 Design of Faults in AHU systems

3.1.1 Operational Modes in an AHU

Typically, there are four primary Modes of operation in the operation sequence of an AHU controller. Sequencing logic determines the Mode of operation as dictated by various thermal relationships including the internal and external loads on the zones served by the AHU. In the heating Mode (Mode 1), heating coil valve is controlled to maintain the temperature of the supply air while cooling coil valve is closed and the dampers for outside air, return air/exhaust air are operating to meet minimum ventilation requirements, which rarely happens except extremely cold climates. When outside air temperature increases, the sequence switches to Mode 2, which closes both heating coil valve and cooling coil valve while controlling the outside air dampers to maintain supply air temperature. Mode 3 is set when cooling coil valve is operating to keep the supply air temperature while using as much outside air as possible for “free cooling”. Then when minimum outdoor air fraction is propped, the sequence is set at Mode 4. Figure 3.1 shows the relationships of Mode 1 through 4 and the operations of AHU components.

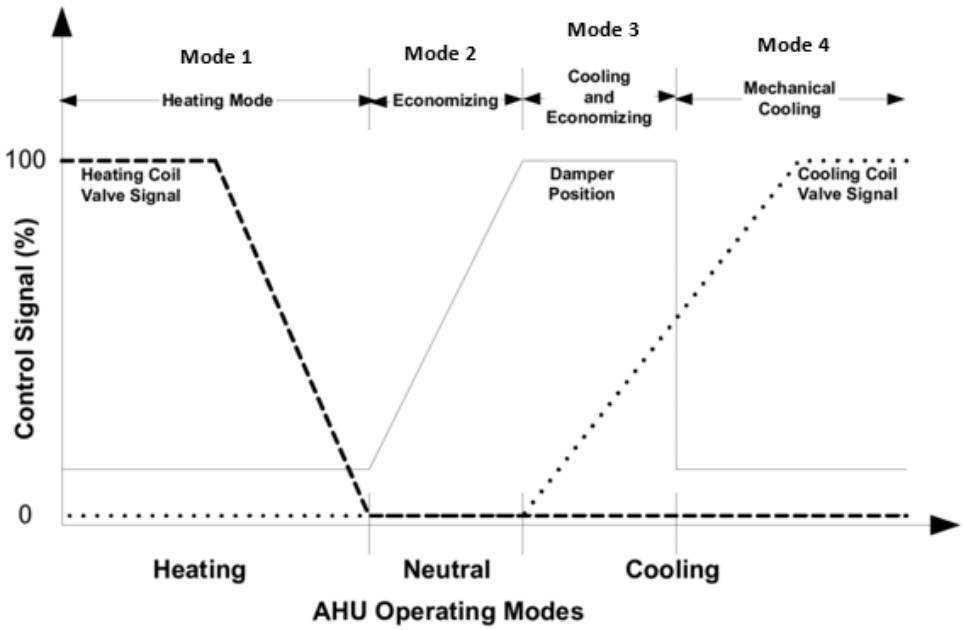

Figure 3.1: Typical operating Modes of AHU [4]

3.1.2 Typical Faults of Air Handling Units and Fault Selection

During operation of the AHU controller discussed previously, any failures in the components, such as the fan, duct, actuators, sensors, etc., can significantly decrease the efficiency of the AHU. Table 3.1 gives a compilation of several typical faults in systems.

Table 3.1: List of Typical Faults on AHU [25]

Category	Device	Typical Faults
Equipment	Fan	Pressure drop is increased Fire damper stuck and increase in resistance Decrease in the motor efficiency Belt slippage
	Duct	Air leakage
	Cooling coil	Fouling (fin and tube) leads to reduced capacity
Actuator	OA, RA, and EA dampers	A damper is stuck or a faulty position is operated Air leakage occurs at fully open and closed positions
	Heating coil valve, cooling coil valve, and preheating coil valve	Valve stuck, broken, or wrong operating position Leakage occurs at fully open and closed positions of the valve
Sensor	SA, MA, OA and RA temperature	Failures of a sensor are offset, discrete or drift

	MA, OA and RA humidity	Failures of a sensor are offset, discrete or drift
	OA, SA, and RA flow rate	Failures of a sensor are offset, discrete or drift
	SA and zone pressure	Failures of a sensor are offset, discrete or drift
Controller	Motor modulation	Unstable response
	Sequence of heating and cooling coil valve	Unstable response
	Flow difference	System stuck at same speed
	Static pressure	Unstable response
	Zone temperature	Unstable response

Out of the list, three faults are selected to be tested and introduced: (1) outside air economizer damper stuck closed, (2) fouling of fin and tube on cooling coil, and (3) fire damper stuck closed affecting the fan. Figure 3.2 shows the faults introduced in their corresponding sections of the AHU system.

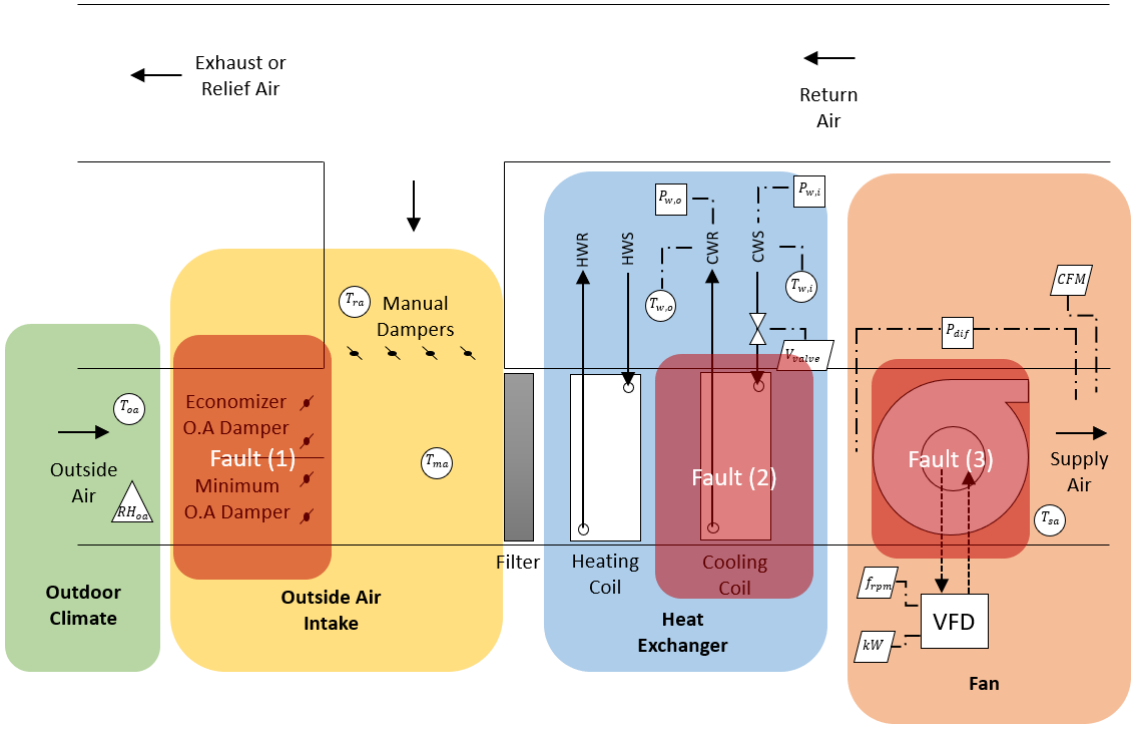

Figure 3.2: Faults located in the corresponding components of the system

3.1.3 Outside Air Intake: Outside air damper fault

Outside air damper fault is critical to the operation Modes as it can provide too much outside air needed or not enough. This excess of outside air can challenge energy savings because hot outside air mixed into the return air results in a greater cooling load to the system. On the other-hand, no outside air can impact human health, as it is unable to meet indoor air quality and ventilation requirements of providing enough outside air to eliminate harmful contaminants and gaseous chemicals. This can also impact the operation sequence of Mode 2 and 3, “free air” process, when outside air is at set point temperature of the supply air and the air does not need any heating or cooling. The reduced amount of outside air in this condition prevents the “free air” operation altogether, not allowing full 100% outside air into the system.

Fully closed outside air damper is introduced into the system. This means that not only can it allow the system to meet ventilation requirements but fully removes operation Mode 2 and 3. APAR rule-based FDD can identify the following faults:

- Stuck or leaking mixing box dampers, heating coil valves, and cooling coil valves;
- Temperature sensor faults;
- Design faults such as undersized coils;
- Controller programming errors related to tuning, setpoints, and sequencing logic;
- Inappropriate operator intervention.

This method is a perfect application for this type of fault.

APAR includes rules of the heating Modes. In this project, the rule-set created by J. Schein et al. are condensed to only distinguish faults during Mode 2, 3 and 4 in

Table 3.2. Also, it has been modified due to the inaccessible measurements such as the supply fan temperature increase and a robust cooling coil valve signal. In addition to this rule-set, the impact of the energy consumption of this fault compared to baseline operation.

Table 2.2: Condensed APAR rule set

Mode	Rule	Rule expression
Cooling with Outdoor air (Mode 2)	1	$T_{oa} < T_{sa} + \varepsilon_t$
	2	$\propto > 0.8 - \varepsilon_{\propto}$
Mechanical Cooling with 100% Outside air (Mode 3)	3	$T_{oa} < T_{ra} + \varepsilon_t$
	4	$0.8 > \propto > 0.2 - \varepsilon_{\propto}$
Mechanical cooling with minimum outdoor air	5	$T_{oa} > T_{ra} - \varepsilon_t$
	6	$\propto < 0.2 + \varepsilon_{\propto}$

3.1.4 **Heat Exchanger: Fouling of cooling coil**

Fouling of cooling coil refers to the accumulation of contaminants on the water-side or air-side of heat transfer surfaces. The fouling increases the thermal resistance and decreases the performance of the equipment. Countless studies of the effects of fouling are published to address the problem. Some of these studies suggest increased pressure drop due to airflow decrease in the system and reduced the thermal conductance, which directly decreases the thermal effectiveness of water-cooled air coils in HVAC systems. [28] [29] The most compelling method to detect this fault is the diminished temperature difference in the water coils due to the reduced thermal effectiveness.

$$\dot{q}_{water-side} = \dot{m} * c_p * \Delta T_{water} \quad (31)$$

Equation 31 describes the heat transfer rate of the water-side. When the thermal effectiveness of the coils decreases, the temperature difference of the inlet and outlet of the chiller water decreases. This introduces the low delta-T syndrome. This phenomenon occurs when the difference between the supply water temperature and the return water temperature is less than design. In order to provide the same amount of heat transfer rate, the mass flow rate must increase which in turn increases the power of the pump to generate enough flow. Some of these cases can consume up to 25% in total. [30]

3.1.5 **Fan: Fire damper stuck**

The performance of the fan heavily relies on the pressure, system resistance, and the volumetric airflow rate. This is due to the governing equation of the fan written as Equation 25 in Chapter 2. When flow through the system increases, the fan head required increases by the square. Similar to the current flow (current can only flow through a resistance by the application of a voltage, flow of air can only be caused to flow through equipment by the pressure drop. Due to the complicated nature of the flow path in equipment, most designers/manufacturers yield to testing the equipment for its resistance characteristics instead calculate the fluid flow equations.

From this testing, the system curve and the fan curve are created for the building HVAC designers to use and select the most suitable HVAC systems to the specific projects. The system resistance, S, is believed to be set. The VFD controls then can monitor the fan speed and manipulate the resulting airflow rate and pressure required to increase efficiency and consume less energy (power) by maintaining the system curve.

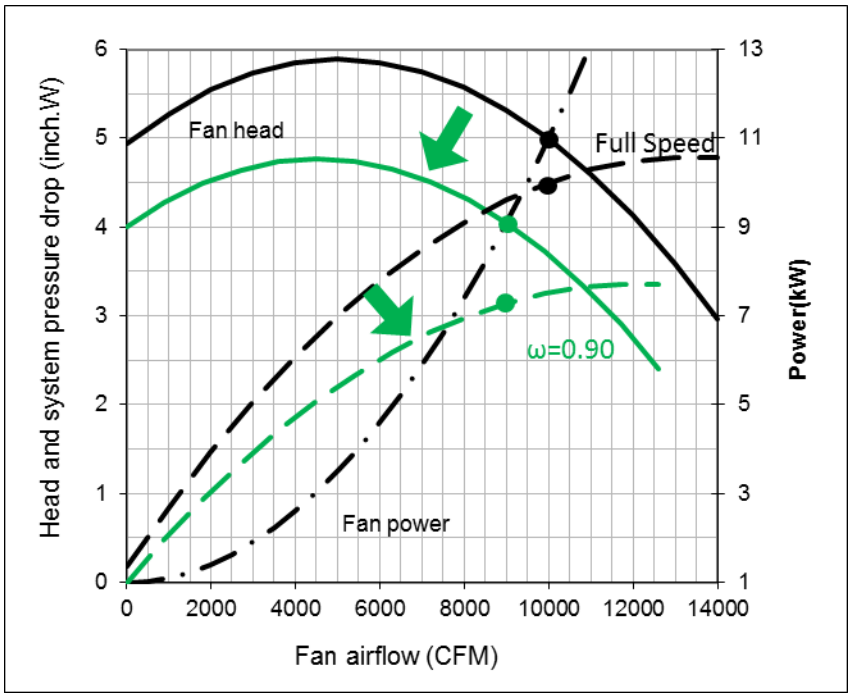

Figure 3.3: A baseline operation of the VFD control regulating the fan speed and the result of changing 100% fan speed to 90% fan speed [26]

When fire dampers are stuck closed and choking the flow of the system, the system resistance increases. When the system resistance increases, the overall fan's efficiency decreases as it maintains the same fan head but generating less airflow rate. This increase the power consumption.

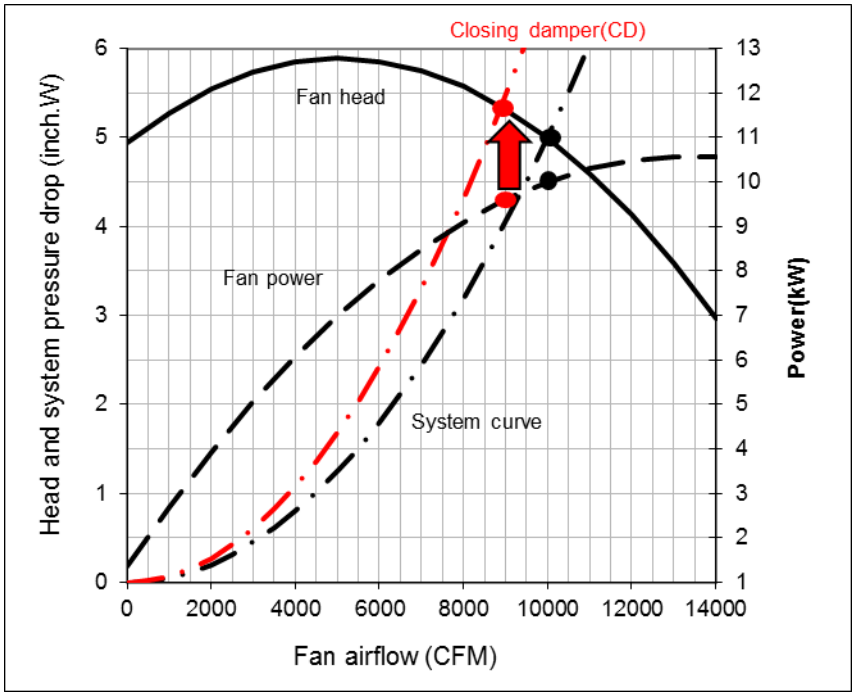

Figure 3.4: A baseline operation of the VAV control regulating air flowrate by closing dampers and representation of the result of stuck closed dampers [26]

FDD for system resistance increase is required for all types of HVAC to maintain energy saving. It is closely studied in this study as the fault is simulated. The FDD program shows a visual comparison of how the fault had changed from its baseline operational duration. Finally, it provides a comparison of the energy consumption of the baseline operation and fault-simulated operation to deliver the effect and significance of the fault.

3.2 Experimental Procedure and Result

Faults are simulated in each sections of the AHU. The experiment procedure and the results are described in detail in this section of the chapter. It also explains the implication of these FDD results and the energy consumption comparison for each of these faults with the baseline operation.

3.2.1 **Blocked/Stuck fully closed outside damper fault**

Outside air damper can affect most during mode 2 and 3 when outside air is utilized as free air. This is when the temperature of the outside air is lower than return air. The fault is simulated during the day when the outside air is lower than return air to represent the importance of this fault to the energy consumption. The set of rules listed are implemented as primary FDD method. The threshold must be set to calibrate the FDD.

ε_t, threshold value of temperature for rules 1, 3, and 5, and $\varepsilon_\propto$, threshold value of alpha ratio for rules 2, 4, and 6, must be set according to the baseline operation of the specific system to correct the rule-based FDD set and match to how the HVAC system operates in its current state before the fault is simulated. The purpose of the threshold values is to create leniency and a wider range to the rules as it analyzes through the data measurements as shown in Figure 3.5.

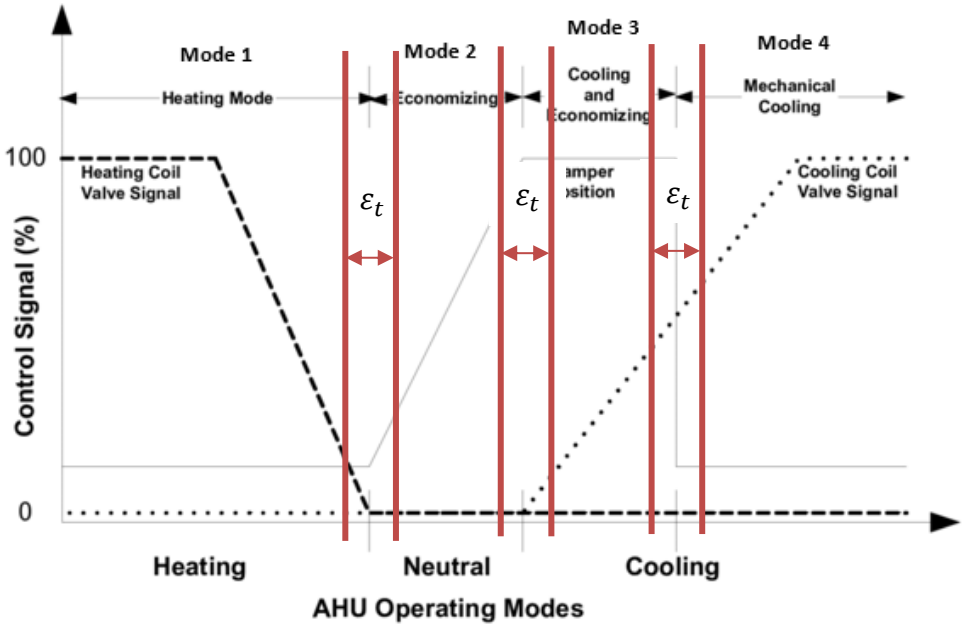

Figure 3.5: Example of the effect of threshold in the rules for detection of operating mode

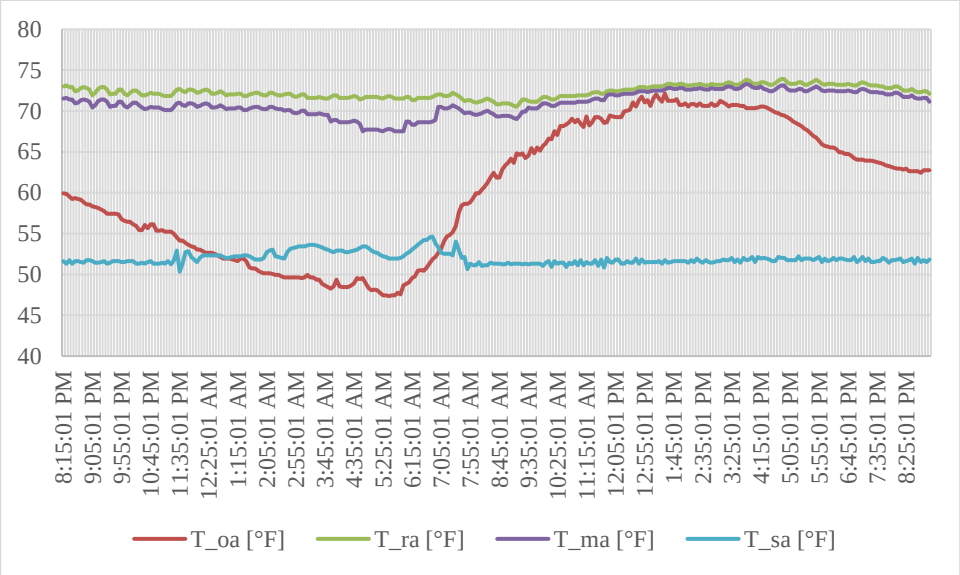

Figure 3.6: Stuck fully closed outside damper fault simulated result of 4/14-15 (accessed in 4/20/19)

Figure 3.7 shows the yellow cell for input. The thresholds are set until the cell under "Any Fault? [Y,N]" indicates N. The thresholds must be also reasonably set without altering the rule. ε_t must be under 5 degrees and $\varepsilon_\propto$ must be under 0.05 for time variance.

Fault-Free Operation													
α	ε_α (rule 2,4,6)	ε_T (rule 1,3,5)	Rule_1	Rule_2	Rule_3	Rule_4	Rule_5	Rule_6	2	3	4	Fault	Any Fault? [Y,N]
0.85547	0.01	4	1	1	1	0	0	0	1	0	0	0	N

Figure 3.7: Baseline operation section with input cell of thresholds

Then, the same set of rules with the thresholds runs through the fault simulated data to test the FDD system. Figure 3.8 depicts the same set ran through the fault simulated data and detecting that there, in fact, is a fault.

Fault Simulated Operation													
α	ε_α (rule 2,4,6)	ε_T (rule 1,3,5)	Rule_1	Rule_2	Rule_3	Rule_4	Rule_5	Rule_6	Mode 2	Mode 3	Mode 4	Fault	Any Fault? [Y,N]
0.076467	0.01	4	0	0	1	0	0	1	0	0	0	1	Y

Figure 3.8: Fault simulated operation section with fault detected

When this fault is present, mode 2 and 3 is eliminated because the outside air cannot be used for the cooling of mixed air. The temperature of mixed air is most likely same as the return air. To visually show the impact of fault in its energy consumption, sensible heat is calculated by using Equation 32.

$$q_{sensible} = 1.1 * Q * (T_{ra} - T_{sa}) \quad (32)$$

Note that the average of volumetric flow rate of the fault free operation, 10800 CFM, is set and utilized in the equation to only assess the difference of the heat transfer due to the temperature difference caused by the damper fault.

The corrected alpha ratio is found in the same faulty data depending on the mode (outdoor air temperature) corresponding to the baseline data. For example, when the outside air temperature measures under 55 degrees, the alpha ratio is corrected to 85% which is given by observing the baseline operation. And when the outside air temperature measures under 75 degrees but greater than 55 degrees, the alpha ratio is corrected to 55%, which is also given by observing the baseline operation. Another sensible heat is calculated and compared.

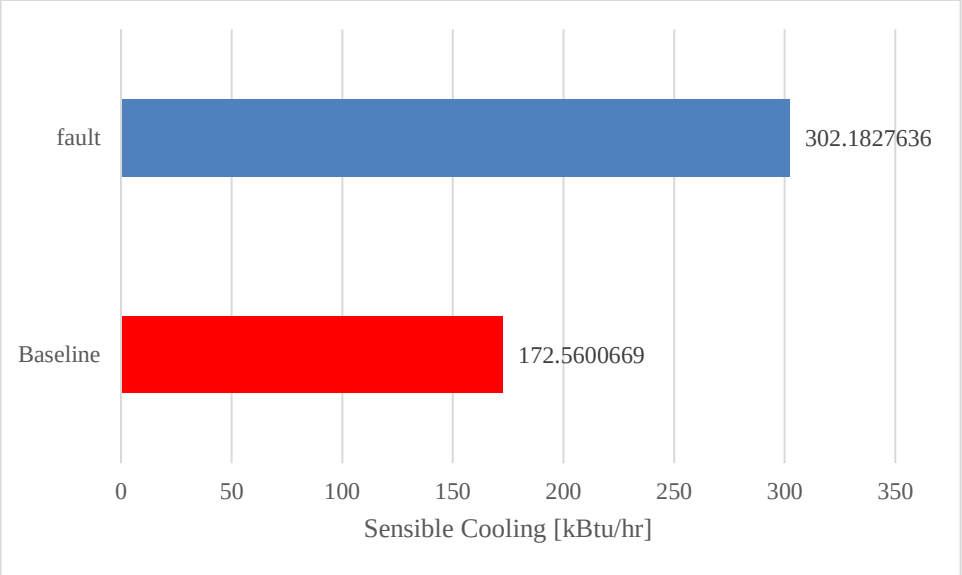

Figure 3.9: Sensible cooling load during baseline operation and fault simulated operation

For this specific time of study, outside air was mostly lower than the return air. In Figure 3.8, baseline operation required 172.56 kBtu/hr of cooling capacity and fault simulated operation needed almost double which is 302.18 kBtu/hr of cooling capacity. This shows the enormous effect on energy consumption due to the outdoor air damper stuck closed. The closed damper limits the AHU to utilize the cold outside air and required to cool the warmer return air in times of mode 2 and 3.

3.2.2 Fouling of Coil

The fouling of coils is simulated by blocking the air entering the coils as the contamination in the coils blocks the air from entering. The blockage reduces the cooling effect due to the lack of surface area for heat transfer. During simulation of the fault, the data is recorded and analyzed which is shown in Figure 3.10. The figure shows that a drastic change in the outlet temperature of the chiller water at 5:30 PM which is when the fault is simulated. The difference of inlet and outlet temperature of the chiller water is decreased and thus the low delta-T syndrome. In the figure, the blue

line indicates an increase when the fouling is introduced to increase the mass flow rate of the water, so it provides enough heat transfer rate from the decrease of delta-T.

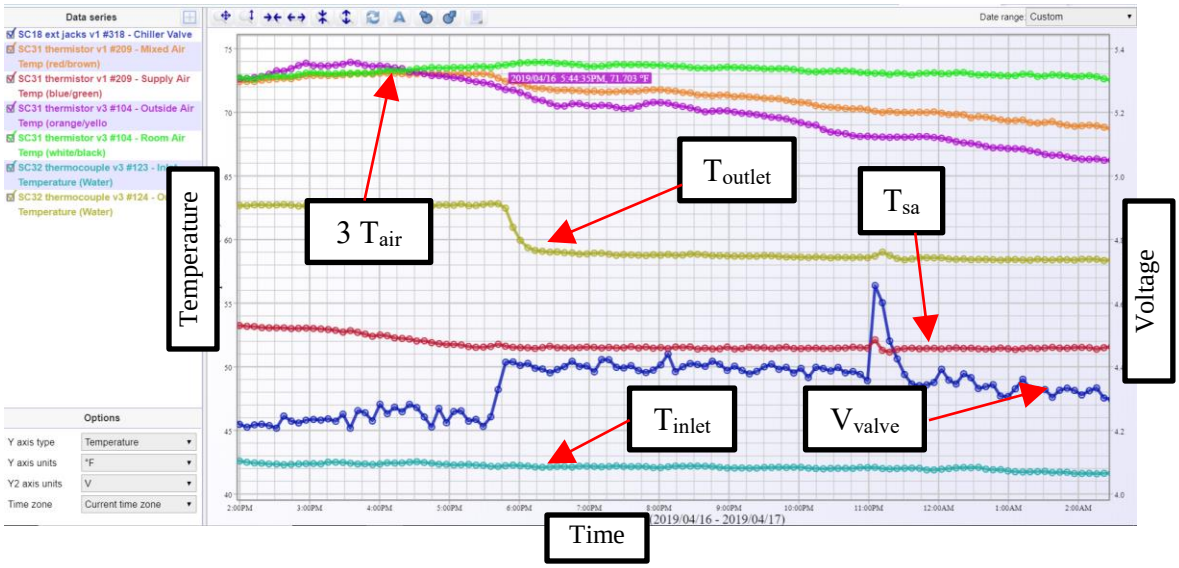

Figure 3.10: Temperature of inlet and outlet of chiller water, position of valve, and air temperature before and after the fouling fault simulation (accessed in 4/17/19)

The FDD program evaluates the temperature difference of baseline data and the fault simulated operation data. It also analyzes the position of the valve. When there is heat transfer (valve position is not closed), then the FDD indicates if there is a decrease in temperature difference of the chiller water during baseline operation and fault simulated operation. Figure 3.11 depicts a portion of the FDD program that indicates if there is a fouling of the cooling coil and the changes of the operation is also provided.

	Change due to Fault		
Fault [Y,N]	**Δ(ΔT)**	**% change_mass flow**	**mean_%_change_mass flow**
Y	-2.849561	0.167666417	0.216732728
Y	-3.499518	0.210238359	
Y	-3.299518	0.197039342	

Figure 3.11: Portion of FDD program that exposes the existence of fouling fault and illustrates the impact of the fault

The fault decreased the temperature difference of the inlet and outlet of cooling coil. Thus, the mass flow rate increased to satisfy the cooling load requirements. The average

percentage rise of mass flow rate, 21.67%, results in an increase of chiller plant power, or an efficiency loss, which can be estimated from the chiller manufacturer's technical data sheet.

3.2.3 Stuck closed fire damper/Overall increase of system resistance

The stuck closed fire damper is simulated by blocking areas inside the AHU equipment. The blockage causes a great amount of noise due to the narrower path that the air must take and the increased air velocity. Figure 3.12 shows a real-time visualization of the pressure required, fan speed, volumetric airflow rate, and the power consumed. The figure shows a change in all categories when the fault is introduced. The airflow rate is minimally decreased indicated by the blue line, fan pressure head is increased shown with purple line, the red line shows an increase in the fan power, and the yellow line indicates the fan speed.

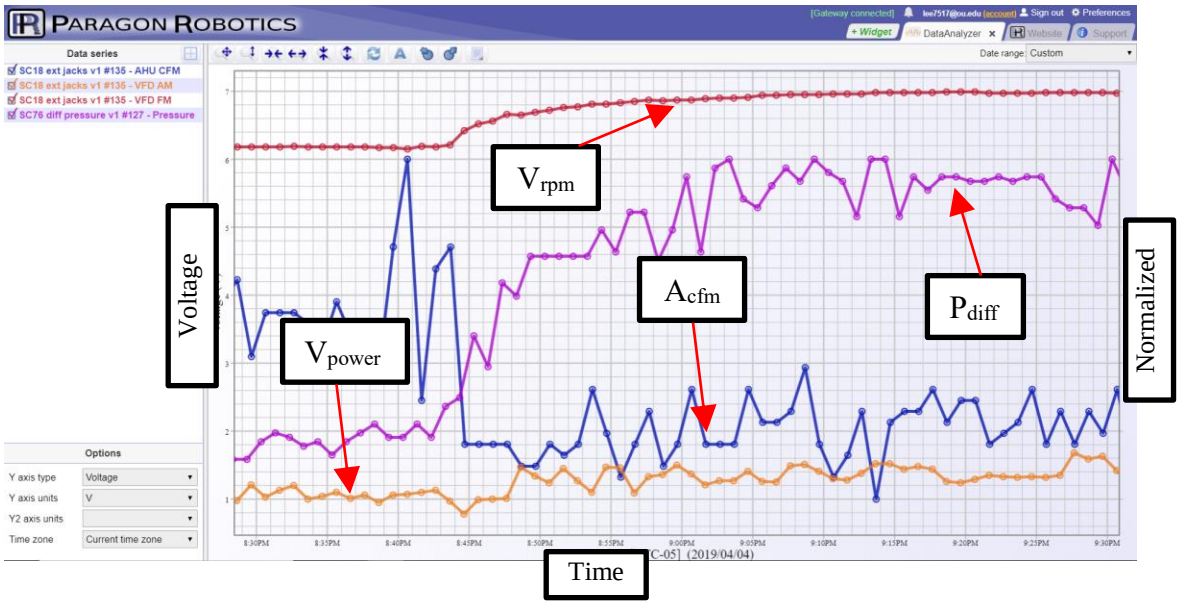

Figure 3.12: Visual representation of the fan parameters during the fault simulated operation in Paragon Robotics website (accessed 4/2/19)

The data from the simulated fault operation duration is loaded into the FDD program. It provides the figure below that indicates the change in the system curve.

Compared to the blue trendline which is the baseline operation system curve, the system curve has shifted to the left which indicates the increase of the system resistance, S.

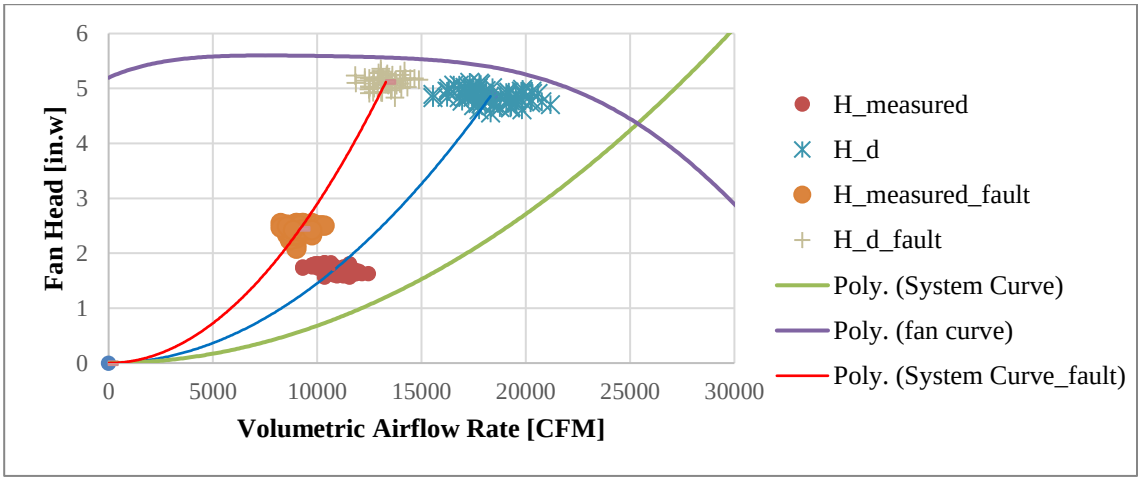

Figure 3.13: System curve of design from manufacturer, baseline, and fault simulated operations

Due to the dynamic changes of the system, a low level of shifting of the system curve can occur, so a threshold is given to provide time delay for any transient properties. The threshold is dependent on the quality and amount of the data from the baseline operation. The mean value of the measured fan head, measured volumetric airflow rate, design fan head and the volumetric airflow rate are calculated to indicate the system curve as well as defining the threshold.

A limit of S values of the baseline condition is given as $S_{threshold}$. When the system curve shifts further left, moving out of the range of baseline condition (or shows a higher value of S compared to the $S_{threshold}$), then it indicates a fault of fire damper stuck closed in the FDD. And as the FDD program indicates the fault, it notifies the operator/user the level of significance of the system as shown in Figure 3.14. Colors of green, yellow and red mean good, okay, and bad condition, respectively. The threshold is set by finding the ratio of S_{mean} of baseline operation to S_{mean} of faulty operation and

calculating the $S_{threshold}$ with the minimum of the volumetric airflow rate with its corresponding fan head (Equation 33). Then, Equation 34 utilizes the threshold to detect if there is an increase of the S value from a fault in the system. The figure indicates that the operation with the simulation of fault is more than 40% divergent from the $S_{threshold}$ of the baseline operation.

$$S_{threshold} = \frac{H_{mean}}{(Q+10\%*Q)^2} \tag{33}$$

$$S_{mean,faulty} > S_{threshold} * (1 + \varepsilon_{fd}) \tag{34}$$

Threshold	Fault [Y/N]	Good	
1%	Yes	Not Optimal	
2%	Yes	Critical	
3%	Yes		
4%	Yes		
5%	Yes		
10%	Yes		
20%	Yes		
30%	Yes		
40%	Yes		
50%	No		
60%	No		
70%	No		
80%	No		
90%	No		
100%	No		

Figure 3.14: A gauge of how critical the fault is by giving a threshold to the S value compared to the S_{max}

After this, to compare the energy spent for 30 days with fault and without fault, the mean of power data, measured directly from the VFD control panel, for both operations were calculated and multiplied by 720 hours, which is a typical duration of filter change/maintenance of HVAC systems. The difference of kWh ratings gives a physical meaning of the effect of the fault. Shown in Figure 3.15, baseline operation

used 3116.96 kWh of power, whereas, faulty operation consumed 4421.14 kWh of power. This type of failure of fire dampers stuck closed can potentially consume more than 40% more power.

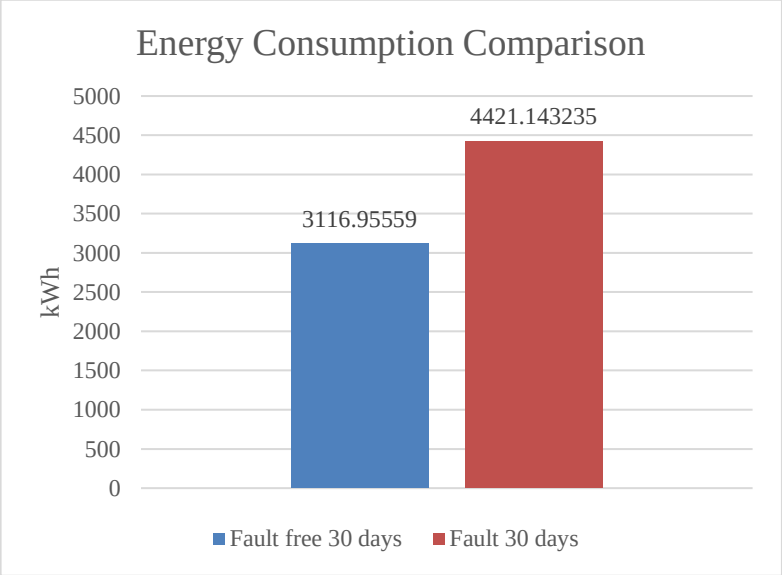

Figure 3.15: Energy consumption of 30 days of baseline and fault simulated operations

Chapter 4: Conclusion and Future Work

In this thesis, an air handling unit with a variable frequency drive control is evaluated. Then, a cloud-based data logging system with appropriate sensors is implemented into the AHU to measure and record different variables. The data logging system is then verified and tested by collected baseline data (existing operation before designed faults are purposely introduced) of the system to assess the current condition. Typical faults of AHU are selected and simulated into the system to collect the faulty data. Faults are detected by a rule-based and data driven method. FDD is created to test the system and energy loss due to the faults are included to indicate the energy saving potential.

The following list summarizes the major works done in the thesis.

1. Literature reviews show various types of FDD methods and usefulness and application purposes of each types. These types are categorized in three: rule-based, data-driven, and model-based. And hybrid techniques, a combination of two or three, have been highly successful and efficient in detecting and diagnosing faults. Although the eminent effectiveness of these studies, applications of FDD in the HVAC industry has not been advancing with the technology of today compared to other industries. Information technology is practical and constructive for the HVAC industry to serve as a main tool to analyze the HVAC systems in depth and control them with greater precision to conserve energy.

2. The AHU is evaluated through the schedules given and the submittals from manufacturing company. Parameters needed to be recorded in the AHU are considered, and corresponding sensors and devices are selected/chosen to assess the condition of the system before any faults. Experimental results are recorded to analyze the AHU and the cloud-based data logging system.

3. Cloud-based data logging system implemented into the system, supplied and manufactured from Paragon Robotics, were easy to handle and robust. Paragon Robotics customer service is outstanding and helpful to locate and solve any problems of the software or hardware. The company responds quickly to inquiries and returning/shipping of devices. The real-time data is examined quickly with Paragon Robotics software on-line or exported and analyzed thoroughly in third-party applications.

   The difficulties that the devices faced in the thesis came from the simplicity of the design. Since the devices does not have any displays but only LED lights, there were problems when the user had to connect and claim the devices on a more complex Internet networks such as the one of University of Oklahoma with greater security. The DataAnalyzer widget has some bugs that were not fixed in the duration of this thesis such as outputting an incorrect value of the difference of two temperatures from thermistors. Lastly, the software developing tool is offered but requires a great amount of knowledge on HTML and JAVA Script coding.

4. Faults of outside air damper stuck closed fully and fire damper stuck fully are simulated to record the measurement information to the cloud and analyze the result of the system. Rule-based/data-driven method is developed. The FDD system is implemented with max energy consumption analysis due to the faults to provide bigger perspective of the problems of the faults.

A new application to cloud-based data logging system was successfully implemented into the AHU system and FDD was validated with the system during this thesis project. Some of future works are still reviewed and listed below to further advance this application.

1. More instruments verifications must be performed with the device. The calibration problem with the water pressure gauge must be identified to deliver robust measurements of the cooling coil flow rate. Also, other sensors such as the Hall Effect liquid flow sensor, ultrasonic flow sensor, and more are to be initiated into the system to provide a wider range of variable measurement techniques and variety of tools associated with the data logging system.

2. FDD methods are implemented through off-line setting by exporting the data measurements onto an external software program. Since the device company has capability of software development in its tools, real-time monitoring can be used for real-time FDD “widget” software developed and implemented.

3. The portability of this device is highly applicable to test other systems. This project can be performed in different types of HVAC systems, such as commercial roof-top units (RTUs), AHU with VAV controls, split systems, and more. The more experiments performed can develop a more robust system and produce greater advancement to the cloud-based technologies.

4. Development of different FDD methods is crucial to progress the project. The cloud-based system can easily implement different FDD methods or already developed methods and test the methods. And these methods can also be compared with each other simultaneously with real-time data and examine the better methods for specific systems.

Chapter 5: References

[1] U. S. Department of Energy, "Saving Energy and Money with Appliance and Equipment Standards in the United States," *Building Technologies Office,* July 2015.

[2] U. S. Energy Information Administration, "Monthly Energy Review," Office of Energy Statistics, Washington DC, 2017.

[3] U. S. Department of Energy, "Energy Consumption Characteristis of Commercial Building HVAC Systems Volume II: Thermal Distribution, Auxiliary Equipment, and Ventilation," Washington, DC, 2001.

[4] J. Schein and S. T. Bushby, "A rule-based fault detection method for air handling units," *Energy and Buildings,* no. 38, pp. 1485-1492, 2006.

[5] D. Claridge, M. Liu and W. Turner, "Whole Building Diagnostics," in *Diagnostics for Commercial Buildings: Research to Practice Workshop*, San Francisco, 1999.

[6] M. Piette, S. Kinney and P. Haves, "Analysis of an information monitoring and diagnostic system to improve building operations," *Energy and Buildings,* no. 33, pp. 783-791, 2001.

[7] TIAX, "Energy Consumption Characteristics of Commercial Building HVAC Systems," U.S. Department of Energy, 2002.

[8] D. Westphalen and K. Roth, "System and component diagnostics," *ASHRAE Journal,* pp. 58-59, 2003.

[9] K. Bruton, P. Raftery, B. Kennedy and M. Keane, "Review of automated fault

detection and diagnostic tools in air handling units," *Energy Efficiency,* pp. 335-351, 21 November 2014.

[10] IEA, "Demonstrating Automated Fault Detection and Diagnosis Methods in Real Buildings," in *Energy Conservation in Buildings and Community Systems ANNEX*, Finland, 2001.

[11] R. Dodier and J. Kreider, "Detecting Whole-Building Energy Problems," in *No. CONF-990102*, University of Colorado, Boulder, 1999.

[12] J. Z. Sikorska, M. Hodkiewicz and L. Ma, "Prognostic modelling options for remaining useful life estimation by industry," *Mechanical Systems and Signal Processing,* vol. 5, no. 25, pp. 1803-1836, 2011.

[13] A. L. Dexter and D. Ngo, "Fault diagnosis in HVAC systems: a multi-step fuzzy model-based approach," *HVAC&R,* vol. 1, no. 7, pp. 83-102, 2001.

[14] T. I. Salsbury and R. C. Diamond, "Fault detection in HVAC systems using model-based feed forward control," *Energy Building,* vol. 33, pp. 403-415, 2001.

[15] B. Yu and S. Riahy, "General modeling for model-based FDD on building HVAC systems," *Simulat. Pract. Theory,* vol. 9, no. 6-8, pp. 387-397, 2002.

[16] J. M. House, H. Vaezi-Nejad and J. Whitcomb, "An expert rules set for fault detection in air handling units," *ASHRAE Trans.*, vol. 107, pp. 858-871, 2001.

[17] J. Schein, S. T. Bushby, N. S. Castro and J. M. House, "A rule-based fault detection method for air handling units," *Energy Buildings,* vol. 38, pp. 1485-1492, 2006.

[18] S. W. Wang and Y. M. Chen, "Fault-tolerant control for outdoor ventialtion air

flow rate in building based on neutral network," *Building Environmental,* vol. 37, no. 7, pp. 691-704, 2002.

[19] W. Y. Lee, J. M. House and N. H. Kyong, "Subsystem level fault diagnosis of a building's air-handling unit using general regression neural networks," *Appliance Energy,* vol. 77, no. 2, pp. 153-170, 2004.

[20] Z. M. Du, X. Q. Jin and Y. Y. Yang, "Wavelet neural network-based fault diagnosis in air-handling units," *HVAC&R Res.,* vol. 14, no. 6, pp. 959-973, 2008.

[21] J. E. Seem, "Using intelligent data analysis to detect abbaseline energy consumption in buildings," *Energy Buildings,* vol. 39, no. 6, pp. 52-58, 2007.

[22] Z. M. Du, X. Q. Jin and L. Z. Wu, "PCA-FDA-based fault diagnosis for sensor fault in HVAC systems," *Energy Conversion Management,* vol. 13, no. 2, pp. 693-702, 2007.

[23] F. Xiao, S. Wang, X. Xu and G. Ge, "An isolation enhanced PCA method with expert-based multivariate decoupling for sensor FDD in air-conditioning systems," *Appli. Therm.,* vol. 29, no. 4, pp. 712-722, 2009.

[24] Z. Du, B. Fan, J. Chi and X. Jin, "Sensor fault detection and its efficiency analysis in air handling unit using the combined neural networks," *Energy and Buildings,* vol. 72, pp. 157-166, 2014.

[25] Y. Yu, D. Woradechjumroen and D. Yu, "A review of fault detection and diagnosis methodologies on air-handling units," *Energy and Buildings,* vol. 82, pp. 550-562, 2014.

Appendix A

Table A-1:Specifications of AHU Cooling Coil and Fan

AHU Cooling Coil		
Variable	**Value**	**Unit**
Total capacity	985.388	kBtu/hr
Sensible capacity	787.244	kBtu/hr
Air flow	25,415	cfm
Max coil velocity	498	fpm
Entering air dry bulb temperature	78.8	^{o}F
Entering air web bulb temperature	63.3	^{o}F
Leaving air dry bulb temperature	50.3	^{o}F
Leaving air wet bulb temperature	49.8	^{o}F
Entering water temperature	42	^{o}F
Water flow rate	145	gpm
Max air pressure drop	0.87	in H2O
Max water pressure drop	7.71	ft
AHU Fan Specifications		
Variable	**Value**	**Unit**
Max air flow	25,415	cfm
Min air flow	9,150	cfm
Motor	30/1750	HP/RPM
Total static pressure	2.5	in H2O
Speed	1,420	rpm
Mechanical efficiency	57	%

Table A-2: Control Valve Schedule

Control Valve		
Variable	**Value**	**Unit**
Water Flow	144.8	GPM
Valve Size	2-1/2	Inch
Shut-Off Pressure	50	Psig
Fail Position	NC	N/A

Appendix B: Air Handling Unit Data Sheet

Temtrol

www.temtrol.com

Unit Data Sheet

Report Created: 4/20/2007 10:37:05AM Submittal 5

Unit Tag: AHU-2
Serial Number: U103054-002-00
Model Number: WF-DH53

Job Name:	OU WAGNER SASC	**Unit Type:**	INDOOR
Rep. Firm:	ENGINEERED EQUIPMENT, INC.	**Unit Weight:**	11174 Lbs.
Rep. Contact:	TRAPPER WILSON @ 525-7722		
Temtrol Eng.:	STA		

Unit Notes

5" Piping sleeves provided by TEMTROL. Located and installed by OTHERS in the field.
L-10 200,000 Hr life bearings.

Unit Details

Exterior Casing: 16 ga. G-90 Galvanized - No Paint
Floor Material: (3/16)-7ga. Alum. Tread Plate ✓
Sub Floor Material: 16ga. Galvanized
Base Size: 2 x 5 x 1/8 in.

Access Doors:

Quantity	Windows	T.O.S.L.	P.K.S.	Louvers
4	0	0	1	0

Static Pressure Summary

Supply

Description	Static
COOLING 5WC - 6 - 36 X 106 X 8 - 10 AL	0.94
4" PLEATED ANGLE 30%	0.60
R/A OPENING	0.10
FACE & BYPASS VIFB	0.25
Internal Static Pressure	1.89
Avaliable External Static Pressure	2.50
Total Supply Static Pressure	4.39

Comment:

Electrical VAC/PH/HZ: 208/3/60

Unless otherwise noted below all electrical and automatic control devices are furnished and installed by others in the field.
Fan motor wired to an exterior mounted junction box.
120 volt power for lighting and/or GFI outlets shall be provided by Others
(See attached cut sheet) Fan access door(s) equipped with a de-energizing switch. Wiring to motor starting device by Others.
Back-to back- j-boxes. (See drawing for locations)

Temtrol

www.temtrol.com

Unit Data Sheet

Report Created: 4/20/2007 10:37:05AM Submittal 5

Unit Tag: AHU-2
Serial Number: U103054-002-00
Model Number: WF-DH53

Job Name:	OU WAGNER SASC	**Unit Type:**	INDOOR
Rep. Firm:	ENGINEERED EQUIPMENT, INC.	**Unit Weight:**	11174 Lbs.
Rep. Contact:	TRAPPER WILSON @ 525-7722		
Temtrol Eng.:	STA		

Unit Notes

5" Piping sleeves provided by TEMTROL. Located and installed by OTHERS in the field.
L-10 200,000 Hr life bearings.

Unit Details

Exterior Casing:	16 ga. G-90 Galvanized - No Paint
Floor Material:	(3/16)-7ga. Alum. Tread Plate ✓
Sub Floor Material:	16ga. Galvanized
Base Size:	2 x 5 x 1/8 in.

Access Doors:

Quantity	Windows	T.O.S.L.	P.K.S.	Louvers
4	0	0	1	0

Static Pressure Summary

Supply

Description	Static
COOLING 5WC - 6 - 36 X 106 X 8 - 10 AL	0.94
4" PLEATED ANGLE 30%	0.60
R/A OPENING	0.10
FACE & BYPASS VIFB	0.25
Internal Static Pressure	1.89
Avaliable External Static Pressure	2.50
Total Supply Static Pressure	4.39

Comment:

Electrical **VAC/PH/HZ:** 208/3/60

Unless otherwise noted below all electrical and automatic control devices are furnished and installed by others in the field.
Fan motor wired to an exterior mounted junction box.
120 volt power for lighting and/or GFI outlets shall be provided by Others
(See attached cut sheet) Fan access door(s) equipped with a de-energizing switch. Wiring to motor starting device by Others.
Back-to back- j-boxes. (See drawing for locations)

Temtrol

www.temtrol.com

Unit Data Sheet

Unit Tag: AHU-2
Serial Number: U103054-002-00
Model Number: WF-DH53

Report Created: 2/8/2007 1:19:29PM Submittal 4

[SUPPLY FAN] AF01-30 / CL II NYB DWDI Housed Airfoil ✓

PHYSICAL		OPERATION	
Motor / Frame / Eff:	30.0hp / 286T / NEMA Pre	Fan CFM @ Alt:	25,415 @ 1,200 ft.
VAC/PH/HZ - RPM / Encl:	208/3/60 - 1750/TEFC	SP @ Alt:	4.36 in. Wg.
Speed / Qty - Belts:	1374 / 4 - BX72	Adj. SP @ Alt:	4.36 in. Wg.
Mtr Max Inertial Load:	687 WR²	SP @ Sea Level:	4.55 in. Wg.
MtrShv / Bushing / Shaft:	4B5V70 / B / 1.875	Fan RPM :	1,381
FanShv / Bushing / Shaft:	4TB90 / Q1 / 2 11/16	Fan BHP / BHP with Belt Loss:	23.44 / 24.17
Isolation / Deflection:	SWERT-2	Static / Mech. Efficiency:	74.4% / 82.3%
Wheel Material / Inertia:	Steel / 93 WR²	Inlet / Outlet Velocity:	2,416 / 2,730 FPM
Direct Drive:	NO		
Max Fan Speed:	1805		

Baldor 10C151X532G2

SOUND OCTAVE BANDS

	63hz	125hz	250hz	500hz	1000hz	2000hz	4000hz	8000hz	A-Weighted
Inlet / Discharge	97 / 97	95 / 95	100/ 100	92 / 92	88 / 88	84 / 84	80 / 80	74 / 74	95 / 95

OPTIONS

Concrete Inertia Base

Comment: CLASS H MOTOR, L-10 200,000 Hr life bearings.

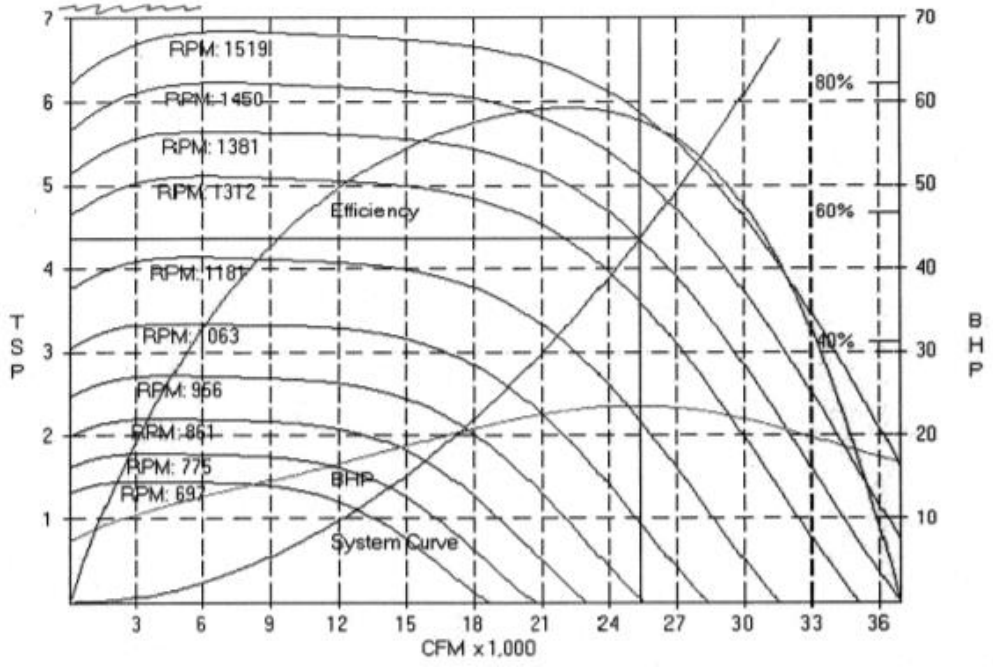

Temtrol

www.temtrol.com

Unit Data Sheet

Unit Tag: AHU-2
Serial Number: U103054-002-00
Model Number: WF-DH53

Report Created: 4/20/2007 10:37:05AM Submittal 5

[Coil # 1] Chilled Water Coil - (Qty. 2) 5WC - 6 - 36 x 106 x 8 - 10 AL

PHYSICAL

Total Face Area / FV :	53.0 / 479.5
Coil FH x FL:	36.00 X 106.00
Rows - FPI:	8 - 10
Serpentine:	1.33
Fin Thickness / Material:	0.008" / AL
Tube O.D. / Wall:	5/8" / 0.025"
Tube Material:	CU
Case Material:	16 GA GALV.
Sup.Conn - Qty / Size:	(1) 2-1/2" MPT SCH40 Red Brass Per Coil
Ret.Conn - Qty / Size:	(1) 2-1/2" MPT SCH40 Red Brass Per Coil
Coating:	NONE

Drain Pan - 116W x 33L 16 GA 304 SS LEFT HAND

Options: Extended Connections

Comment:
1. ARI CERTIFIED 'Rated in Accordance with ARI Standard 410'

OPERATION

ACFM / SCFM - Alt.:	25,415 / 23,577 - 1,200 ft.
EDB / EWB:	78.8 / 63.3 °F
LDB / LWB:	48.4 / 48.3 °F
Total Heat:	1,014,836 Btu/Hr
Sensible Heat:	787,650 Btu/Hr
Fluid - %:	Water
EFT / LFT:	42 / 55.9 °F
GPM:	145.00
Fluid Velocity:	2.60 ft/s
FPD:	7.06 ft
APD:	0.94 in. Wg.
Hand:	LEFT

COILS

[Filter Bank # 1] Pre - 4" Pleated Angle - 30%

Type: Angle **Frames:** Galvanized **Location / Service:** Up Stream / Side Load
Bank Size: 78 H x 96 W **(Qty) Size:** (20)24x24
Face Area (ft²) / FV (fpm): 80.0 / 318
Filter Bank Gauge: Dwyer Model 2001
Media - Pre Filter **APD:** 0.50 **Class:** II **Supplied Sets:** No Media **Clips:**
Comment: Filter frames by Temtrol. Pre Filter media and holding clips are furnished by others.

[UDC # 1] Face & Bypass VIFB - *

APD: 0.25 in. Wg.

Manufacturer	Wing	**Hand**	LEFT
Model	VIFB -VC-8 1 ROW		
CFM	9150 CFM		
EDB to LDB (Degree F)	29.3° to 76.7°		
BTU/Hr	448,919		
Operator (Elec / Pneum)	ELEC.		
Comment:	5" Piping sleeves provided TEMTROL. Installed by OTHERS in the field.		

Openings

Description	Size (A x B)	Location	CFM	FV
R/A	96 x 30	Top - No Duct Flange	25415	1,270
S/A FAN	40.5 x 33.5	End - Discharge - No Duct Flange	25415	2,730